Journal of
Polymer & Composites

https://journals.stmjournals.com/jopc

ISSN: 2321-2810 (Online)
ISSN: 2321-8525 (Print)
Volume 14, Special Issue 4, 2026
January–December
DOI (Journal): 10.37591/JoPC

Research JoPC

Neuromorphic Self-Learning Polymer–MXene Photovoltaic Composites with Embedded Memristive Energy Routing for Adaptive Solar Energy Harvesting

Ajoy Kumar Nandy[1,*], Rajkumar Jhapte[2], Vishal Moyal[3], V. Vinodhini[4], Mahendra Kumar R.[5], D. Suresh[6], Yogesh Diliprao Sonawane[7]

Abstract

This dynamic and fast-growing intelligent renewable energy system requires photovoltaic materials that can autonomously adapt to fast-changing environmental conditions. In this study, a novel system is proposed for adaptive harvesting of solar energy based on Neuromorphic Self-Learning Polymer–MXene Photovoltaic Composites (NSPMPCs) with embedded memristive energy routing networks. To boost the charge generation and charge transport in the polymer–MXene heterostructure, the flexibility and processability of conductive polymers are integrated with the extraordinary electrical conductivity, surface chemistry, and photothermal properties of MXene nanomaterials. The embedded memristive architecture learns continuously the variations of the irradiance, shading patterns and load variations, dynamically reconfiguring the energy pathways inside the device to optimize the power extraction and minimize the conversion losses. The proposed routing mechanism is a neuromorphic one that allows for self-optimization without external supervising control, thus increasing the energy-conversion efficiency, response speed and operational reliability of the system, even in the presence of non-uniform illumination. Adaptive power tracking, energy retention and long-term stability are significantly improved using simulation studies when compared with conventional PV composites. The proposed framework paves the way for the development of next generation of PV materials which will be able to learn, heal and dynamically manage energy to form sustainable energy infrastructure.

Keywords: Neuromorphic photovoltaics, Adaptive solar energy harvesting, Polymer–MXene composites, Memristive energy routing, Self-learning energy systems

***Author for Correspondence**
Ajoy Kumar Nandy
E-mail id: dran_mech@vignan.ac.in

[1]Assistant Professor, Department of Mechanical Engineering, Vignan's Foundation for Science, Technology & Research (Deemed to be University), Vadlamudi, Guntur, Andhra Pradesh, India
[2]Associate Professor, Department of Electrical Engineering, STME, SVKM NMIMS Global University, Dhule, Maharashtra, India
[3]Professor, Department of Electrical Engineering, STME, SVKM NMIMS Global University, Dhule, Maharashtra, India
[4]Associate Professor, Department of Electronics and Communication Engineering (ECE), Saveetha School of Engineering, Saveetha Institute of Medical and Technical Sciences (SIMATS), Chennai, Tamil Nadu, India
[5]Assistant Professor, Department of Computer Science and Engineering, Vel Tech Rangarajan Dr. Sagunthala R&D Institute of Science and Technology, Chennai, Thiruvallur, Tamil Nadu, India
[6]Assistant Professor, Department of Mechanical Engineering, Indra Ganesan College of Engineering, Trichy, Tamil Nadu, India
[7]Assistant Professor, Department of Mechanical Engineering, School of Technology Management and Engineering, SVKM's NMIMS Global University, (formerly Shri Vile Parle Kelavani Mandal's, Institute of Technology), Dhule, Maharashtra, India

Received Date: July 25, 2026
Accepted Date: July 29, 2026
Published Date: August 01, 2026

Citation: Ajoy Kumar Nandy, Rajkumar Jhapte, Vishal Moyal, V. Vinodhini, Mahendra Kumar R., D. Suresh, Yogesh Diliprao Sonawane. Neuromorphic Self-Learning Polymer–MXene Photovoltaic Composites with Embedded Memristive Energy Routing for Adaptive Solar Energy Harvesting. Journal of Polymer & Composites. 2026; 14(Special Issue 4): S453–S488p.

INTRODUCTION

With the growing global demand for sustainable energy production, and the intermittent nature of sunlight, the development of intelligent PV materials that can adjust to changing environmental conditions is highly encouraged. Traditional PV systems are mostly dependent on power electronic controllers and maximum power point trackers outside the PV module to maximize energy extraction from the module in a changing environment of irradiance, temperature and partial shading. Despite considerable progress in photovoltaic materials and energy management strategies, the current PV systems are still passive and cannot autonomously learn from their surroundings and adapt their own energy management strategies. The recent advances of neuromorphic engineering, memristive computing and two-dimensional nanomaterials provide new possibilities for developing cognitive energy harvesting platforms based on biological neural systems. The superior electrical conductivity, high carrier mobility, controllable surface functionalization and outstanding photothermal properties make MXenes an ideal choice for next generation PV devices. At the same time, conductive polymer matrices possess mechanical flexibility, lightweight properties, and are easily fabricated in large areas which allows us to realize flexible and wearable energy harvesting devices. The incorporation of MXene nanosheets into polymer photovoltaic composites leads to synergic effects; this increases the efficiency of charge separation, reduces recombination loss and increases the energy conversion performance. Moreover, the inclusion of memristive energy routing components into these materials brings in the ability of the material itself to adaptively change energy routing pathways based on historical irradiance profiles and load requirements – a learning behavior. These self-learning, neuromorphic energy routing, distributed decision-making and adaptive power optimization systems allow a power system to operate without any central control systems. This proposed Neuromorphic Self-Learning Polymer–MXene Photovoltaic Composite architecture thus introduces a paradigm shift from traditional PV materials to intelligent energy materials that can learn, remember, optimize and function resiliently. The properties make this technology a promising technology for a smart grid, autonomous sensor networks, wearable electronics, Internet of Things ecosystems and next generation sustainable energy infrastructures.

New advances in neuromorphic materials, MXene nanostructures and smart energy systems have led to the rapid progress of adaptive PV technology that combines sensing, memory and computation into one material platform. The material's excellent conductivity, tunable surface terminations and flexibility of fabrication make it ideal to integrate sensing, memory and computing elements, all in one, into low-power systems, which has generated a significant interest in MXenes for applications in neuromorphic computing and memristive systems [1]. MXene-based composites have also exhibited very promising properties in energy harvesting and storage devices, owing to the superior charge transport properties and electrochemical stability [2]. Combining MXenes with polymeric substrates has allowed the creation of flexible optoelectronic synapses and artificial neurons that can mimic the learning behavior of biological neurons for adaptive electronics applications [3]. MXene nanocomposites have demonstrated enhancements in light absorption, carrier separation efficiency, thermal stability, and power conversion in next-generation solar devices for photovoltaic technologies [4]. The recent progress of algorithmic learning methodologies has also inspired the development of self-optimizing energy systems that are capable of self-organization under conditions of uncertainty for their operation [5]. In recent years, the study of MXene-based neuromorphic sensors and intelligent computing architectures has shown its compatibility with edge intelligence and distributed cognition application [6, 7]. Adaptive energy routing systems have been shown to have non-volatile learning and synaptic plasticity in flexible MXene memory devices and neuromorphic architectures [8]. The computation overhead and energy consumption of embedded intelligence platforms have also been further lowered by phase-change memories and analog-in-memory computing methods [9, 10]. Furthermore, the combination of 2D materials and memristive technologies has paved a promising avenue for the design of highly efficient neuromorphic hardware-based systems [11]. The identification of stable MAX and MXene phases for electronic and photovoltaic applications has been sped up using machine learning-assisted material discovery [12]. Extensive studies have demonstrated the ability of the MXene memristors to demonstrate analog switching, multi-level conductance and long-term memory effects required for synaptic computation [13]. The synthesis protocols of Ti(_3)C(_2)T(_x) MXenes have now been established to produce materials with enhanced reproducibility and device scalability [14], and flexible memristors with engineered MXene nanosheets have shown to have an efficient performance of neuromorphic computation at low voltages [15]. Adaptive resistance modulation and analogue learning behavior have also been realized with chemically configurable MXene memristors [16]. In this regard, the use of artificial intelligence has been shown to grow in significance for the realization of modern renewable energy infrastructures, both in nonlinear signal processing [17] and in floating photovoltaic systems [18], as well as in GaN device modelling [19] and in the development of intelligent solar monitoring [20] and energy harvesting optimization [21] and autonomous energy management [22–25]. Specifically, machine learning has boosted PV energy harvesting efficiency and monitoring [20] and Markov decision process-based approaches in energy management have optimized the performance of renewable microgrids under uncertainty [22]. The adaptive environmental response mechanisms in enhancing solar conversion efficiency have also been confirmed by experimental investigations on solar PV temperature reduction with water cooling and color filtering [25].

Figure 1 illustrates the proposed research workflow for developing Neuromorphic Self-Learning Polymer–MXene Photovoltaic Composites with embedded memristive energy routing for adaptive solar energy harvesting. The process begins with problem definition and objective formulation, focusing on the limitations of conventional photovoltaic systems in handling dynamic environmental conditions and the need for self-learning energy routing mechanisms. Subsequently, a comprehensive literature review identifies research gaps associated with MXene materials, memristive devices, and neuromorphic energy systems. The material design and fabrication stage involves MXene synthesis, polymer composite preparation, and integration of memristive networks into photovoltaic structures. Structural, electrical, optical, and thermal characterization techniques are then employed to evaluate material and device properties while establishing mathematical and neuromorphic learning models. Simulation studies assess photovoltaic efficiency, memristive switching behavior, and adaptive energy routing performance under varying operating conditions. Finally, experimental validation and comparative analysis verify the effectiveness of the proposed architecture, demonstrating its capability for intelligent, self-adaptive, and autonomous solar energy harvesting. Despite these improvements, the current PV systems still manage energy harvesting, memory, computing and control as separate components, each controlled by an external controller and relies on an external communication network. Today, however, no solar technology exists that has the intrinsic ability to learn environmental patterns and dynamically reconfigure internal charge transport pathways. Thus, the major issue discussed in this work is the lack of any neuromorphic photovoltaic material that incorporates self-learning, memory retention and adaptive energy routing within the energy harvesting material. To address this limitation, the proposed Neuromorphic Self-Learning Polymer–MXene Photovoltaic Composite with Embedded Memristive Energy Routing aims to integrate PV conversion, synaptic memory and power routing intelligent functionalities within a single, adaptive and autonomous solar energy harvesting cognitive material architecture.

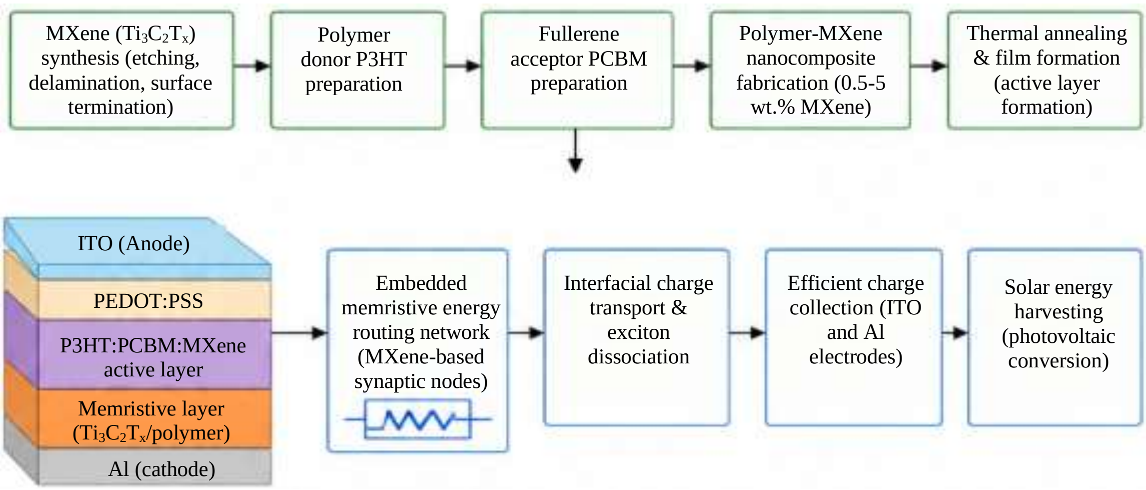

Figure 1. Workflow for developing polymer–MXene photovoltaic composites.

Figure 2 presents the material design and multilayer architecture of the proposed Neuromorphic Self-Learning Polymer–MXene Photovoltaic Composite (NSPMPC). The figure highlights the incorporation of $Ti_3C_2T_x$ MXene nanosheets and P3HT donor–acceptor polymers within a flexible photovoltaic platform fabricated on an ITO-coated PET substrate. The active layer contains interconnected MXene conductive pathways and embedded memristive junctions that provide synaptic learning and adaptive energy routing capabilities. PEDOT serves as the hole transport layer, while silver electrodes enable efficient charge collection. A transparent fluorinated polymer encapsulation layer protects the device from oxidation and moisture without compromising optical transmission. The FESEM and AFM images confirm the formation of exfoliated MXene nanosheets, homogeneous nanocomposite morphology, and smooth surface topography, whereas the cross-sectional micrograph validates the uniform multilayer stacking essential for stable photovoltaic operation and neuromorphic functionality.

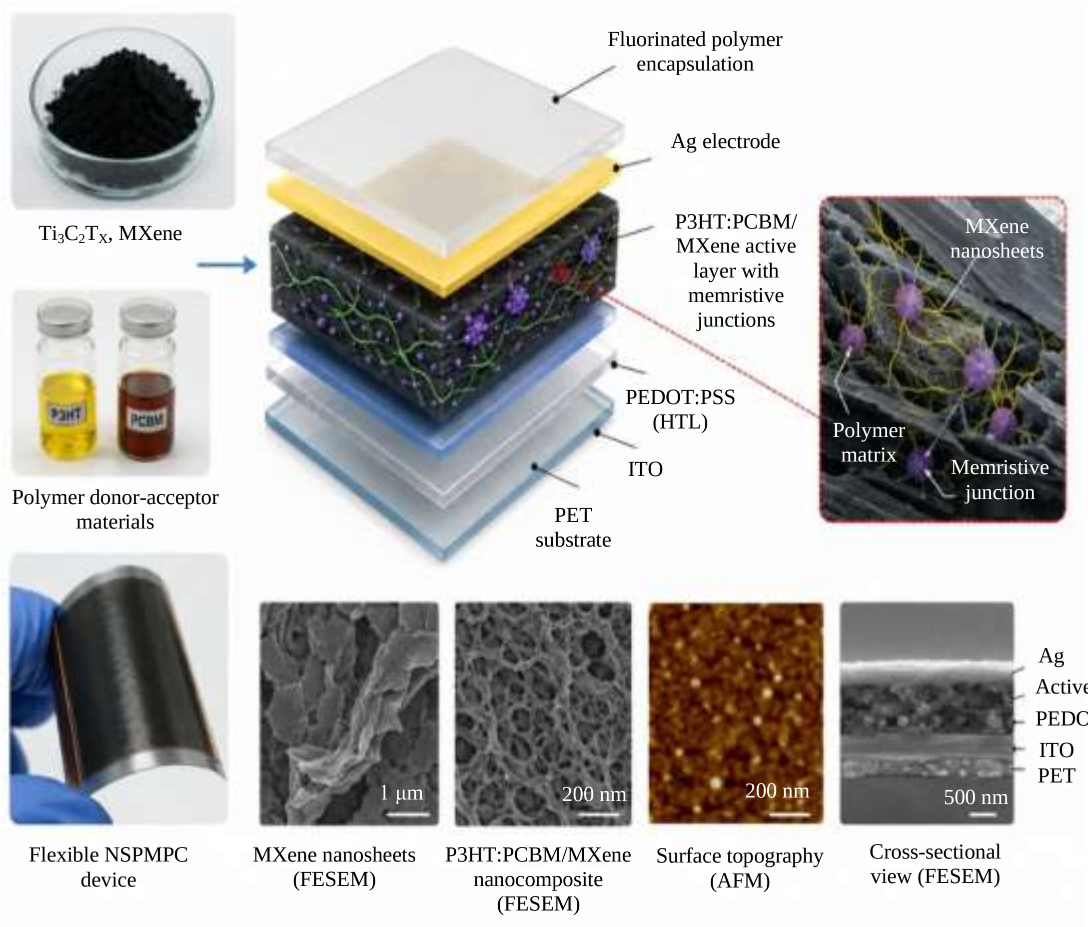

Figure 2. Material design and multilayer architecture of the proposed research.

MATERIALS AND NANOCOMPOSITE DESIGN

MXenes are 2D nanostructures composed of transition metal oxides that possess excellent electrical conductivity, electrical storage, and photoconversion capabilities. The flexible semiconducting polymer matrix, with embedded energy routing interfaces that are memristive, were incorporated into a single composite design to engineer a multifunctional intelligent nanocomposite that simultaneously functions as a photoconversion device, a memory device, and an energy manager. $Ti_3C_2T_x$ was chosen as the representative MXene family as it has superior metallic conductivity, surface chemistry, also high carrier mobility and is hydrophilic, and has good compatibility with polymer solution processing methods. A few-layer $Ti_3C_2T_x$ nanosheets with a high surface area and surface functional groups (such as –OH, –O, and –F) were prepared by selectively etching the Al layers from Ti_3AlC_2 MAX phase precursors and delaminating using intercalation. These functional terminations led to a good interfacial interaction with the polymer chains, and enhanced charge transfer through the hybrid interface. The bulk heterojunction (BHJ) blend of poly(3-hexylthiophene) (P3HT) and [6, 6]-phenyl-C_{61}-butyric acid methyl ester (PCBM) was chosen as the active photovoltaic (PV) medium because they are known to efficiently separate charges, mechanically flexible, low-temperature processable, and suitable for large-area thin film fabrication. The introduction of $Ti_3C_2T_x$ nanosheets into the P3HT: PCBM matrix created interconnected conductive channels which facilitated the extraction of carriers, decreased the recombination of trap-assisted carriers, and increased the dissociation of excitons under solar light. The concentration of MXenes loaded into the polymer (0.5–5 wt.%) was optimized so the electrical conductivity and optical transparency were well balanced, and if the amount of loaded nanosheet was too high, it would absorb light and aggregate, which would interfere with the performance of the photovoltaics. The fabrication of the nanocomposite involved the exfoliation and dispersion of the MXene nanosheets in dimethyl sulfoxide (DMSO) using ultrasonic exfoliation and solution blending with polymer precursors, with continuous magnetic stirring to achieve a homogeneous distribution of MXene nanosheets throughout the matrix. The resulting suspension was spin coated onto indium tin oxide coated flexible polyethylene terephthalate substrates and the films were thermally annealed under controlled conditions to enhance molecular ordering, phase separation, and crystallinity of the films.

Major synthesis, interfacial interaction, charge transfer and thermal stabilization reactions of the Neuromorphic Self-Learning Polymer–MXene Photovoltaic Composite (NSPMPC) can be represented using the chemical design equations.

Selective Etching and MXene Formation

The $Ti_3C_2T_x$ MXene nanosheets are synthesized from the MAX phase precursor Ti_3AlC_2 through selective removal of Al layers:

$$Ti3AlC2 + 3HF \rightarrow Ti3C2 + AlF3 + \frac{3}{2}H2$$

Subsequent surface functionalization produces the terminal groups responsible for high conductivity and interfacial activity:

$$Ti3C2 + xH2O + yOH - +zF - \rightarrow Ti3C2Tx$$

where

$$Tx = (-OH, -O, -F)$$

The surface terminations improve wettability, charge transport, and polymer compatibility.

Polymer Donor–Acceptor Exciton Generation

Upon photon absorption by P3HT, excitons are generated within the donor phase:

$$P3HT + hv \rightarrow P3HT^{*}(e - +h+)$$

where *hv* represents incident photon energy and $P3HT^{*}$ denotes the excited excitonic state.

Interfacial Charge Separation

The generated exciton dissociates at the P3HT/PCBM interface:

$$P3HT^{*} + PCBM \rightarrow P3HT + +PCBM^{-}$$

This process creates free charge carriers responsible for photocurrent generation.

MXene-Assisted Electron Transfer Pathway

The electron captured by PCBM is transferred to the conductive MXene network:

$$PCBM - + Ti3C2Tx \rightarrow PCBM + Ti3C2Tx(e-)$$

The MXene nanosheets provide ultrafast electron transport pathways and reduce recombination losses.

Charge Collection at Electrodes

The extracted carriers are transported toward the electrodes:

$$Ti3C2Tx(e-) \rightarrow ITO/PET + e -$$

$$P3HT + \rightarrow hanode +$$

This reaction contributes directly to photovoltaic current generation.

Thermally-Assisted Polymer Ordering

Thermal annealing promotes crystallization and phase segregation:

$$P3HTamorphous \xrightarrow{120-150\circ C, 15-30min} P3HTcrystalline$$

The process increases carrier mobility and improves photovoltaic efficiency.

Memristive Junction Redox Switching

The neuromorphic switching mechanism can be represented by reversible ionic migration:

$$M0 \rightleftharpoons M + + e -$$

followed by conductive filament formation:

$$nM + + ne - \rightarrow Mn$$

where M denotes mobile metallic species responsible for memristive conductance modulation and synaptic learning behavior.

Moisture and Oxidation Protection

The encapsulation layer suppresses oxidation reactions:

$$Ti3C2Tx + O2 + H2O \rightarrow TiO2 + COx$$

The barrier layer minimizes this degradation pathway, thereby improving long-term device stability.

Electro-Thermal Heat Dissipation

The heat generated during operation is dissipated through the composite matrix according to:

$$Qgen = Qcond + Qconv + Qrad$$

or equivalently,

$$I2R = k\nabla T + h(T - Tamb) + \varepsilon\sigma(T4 - Tamb4).$$

The overall energy conversion process in NSPMPC may be summarized as:

ISSN: 2321-2810 (Online) ISSN: 2321-8525 (Print)

$$hv + \frac{\frac{P3HT}{PCBM}}{Ti3C2Tx} \rightarrow Electrical\ Energy + Heat$$

The nanocomposite operation may be summarized by the coupled reaction sequence:

$$Ti3AlC2 \rightarrow Ti3C2Tx \rightarrow (P3HT/PCBM/Ti3C2Tx) + hv \rightarrow e - +h+\rightarrow Pelectrical + \Delta Gsynaptic + Qthermal$$

All of these chemical equations collectively outline the synthesis of the MXenes, generation of excitons, separation of charges, transport of charges, learning mechanism in the form of memristor, and the suppression of degradation and thermal stabilization when the proposed Neuromorphic Self-Learning Polymer–MXene Photovoltaic Composite (NSPMPC) system is operated.

Nanoscale junctions of partially oxidized MXene interfaces were introduced along conductive pathways to integrate with the rest of the composite to create neuromorphic functionality. These junctions demonstrated analog resistance modulation, conductance plasticity, and multilevel switching states that are like biological synapses, allowing local storage of information and adaptive decision making, based on historical illumination patterns and load conditions. The memristive network was constantly sensing current routes and automatically altering internal resistance states to reroute electrical energy onto energetically preferred paths under irradiation changes, mismatch and partial shading situations. This adaptive routing behavior reduced energy harvesting efficiency losses due to resistive losses, avoided hotspot formation, and reduced the loss without the need of any external supervisory control algorithm. Moreover, the polymer matrix offered flexibility, mechanical strength, environmental durability, and the nanosheets of MXenes added an increased thermal conductivity to enable passive heat transfer and reduce efficiency loss due to temperature effects. Further, the active layers were protected from oxidation, UV exposure and water penetration by the addition of transparent fluorinated polymer encapsulation layers. As a result, the overall NSPMPC architecture combined PV generation, synaptic memory, adaptive energy routing, and thermal management, and paved the way for a paradigm change from passive solar materials to autonomous, solar-powered materials that are capable of self-learning, self-optimization, and autonomous processing of energy in the next generation of smart energy infrastructures.

For the proposed NSPMPC architecture, the material design parameters presented in Table 1 were chosen to optimize the PV conversion efficiency, the neuromorphic learning capability and the long-term operational stability of the NSPMPC. The loading of $Ti_3C_2T_x$ MXenes was limited to 0.5–5 wt.% to ensure good conductive pathways and also optical transparency for photon absorption. The bulk heterojunction of P3HT:PCBM was used as the active photovoltaic medium, which has been found to have excellent exciton dissociation and charge transport properties.

Good light harvesting with minimal recombination losses were obtained with an active layer thickness of 180–250 nm. Thermal annealing at 120–150°C enhanced the crystallinity of the polymer and enhanced charge transfer at the interface, which led to analog conductance modulation and synaptic operation of nanoscale memristive junctions of 20–50 nm size for adaptive energy routing. Moreover, the reliable self-learning operation of photovoltaics (PVs) under different environmental conditions was achieved due to fluorinated encapsulation layers and enhanced thermal conductivity of MXenes. Also, the operation of photovoltaics (PVs) was reliable in a self-learning module under different environmental conditions, thanks to the fluorinated encapsulation layers and enhanced MXene thermal conductivity.

Table 1. Material design parameters of the neuromorphic self-learning polymer–mxene photovoltaic composite (NSPMPC).

Parameter	Symbol/unit	Selected value	Function in nanocomposite design
MXene Material	–	$Ti_3C_2T_x$	High electrical conductivity and carrier transport.
MXene Concentration	wt.%	0.5–5.0	Balances conductivity and optical transparency.
MXene Layer Thickness	nm	2–5	Provides large surface area and interfacial interaction.
Polymer Donor Material	–	P3HT	Photon absorption and hole transport.
Polymer Acceptor Material	–	PCBM	Electron transport and charge separation.
Solvent for MXene Dispersion	–	DMSO	Uniform nanosheet dispersion.
Substrate Material	–	ITO/PET	Flexible transparent conductive support.
Active Layer Thickness	nm	180–250	Optimizes light absorption and carrier extraction.
Spin Coating Speed	rpm	1500–2500	Controls film uniformity and thickness.
Thermal Annealing Temperature	°C	120–150	Enhances crystallinity and phase separation.
Thermal Annealing Time	min	15–30	Improves molecular ordering.
Memristive Junction Size	nm	20–50	Enables synaptic resistance switching.
Encapsulation Layer Thickness	μm	5–10	Moisture and oxidation protection.
Thermal Conductivity	$W\ m^{-1}\ K^{-1}$	2.5–5.2	Passive heat dissipation capability.
Operating Temperature Range	°C	–20 to 85	Stable photovoltaic operation.

The entire fabrication process of the proposed Neuromorphic Self-Learning Polymer–MXene Photovoltaic Composite (NSPMPC) on the experimental platform with white background is shown in Figure 3. The first step involves preparing $Ti_3C_2T_x$ MXene powder, which is then exfoliated, along with stable suspension of few-layer nanosheets, by ultrasonically processing the powder in dimethyl sulfoxide. The homogeneous distribution and no agglomeration of the nanosheets obtained by subsequent magnetic stirring results in better contact of the two interfaces in the composite matrix. The semiconducting polymer components, P3HT and PCBM, are then dispersed in the MXene solution and stirred evenly to yield a uniform polymer–MXene solution that exhibits an optimized charge transport property. This nanocomposite precursor is then deposited on a flexible indium tin oxide coated polyethylene terephthalate substrate by spin coating allowing for exact control of the film thickness and surface uniformity. Thermal annealing at 120–150°C allows the polymer to crystallize, optimize the polymer phase separation and improve the mobility of the carriers. A controlled partial oxidation of MXene interfaces is then followed to create analog resistance switching synaptic learning behavior and memristive junctions. Finally, transparent fluorinated polymer layers are used to encapsulate the fabricated PVs to prevent oxidation and moisture penetration and to maintain optical transparency and stability over practical environmental conditions.

Synthetic Ti_3AlC_2 MAX phase powder (325 mesh, ≥98% purity) was used as a precursor for the synthesis of MXenes. The photoactive materials used were Poly(3-hexylthiophene) (P3HT, 96% regioregularity, 50–70 kDa, electronic grade, Sigma–Aldrich) and PCBM (99.5%, Solenne BV) in a 1:1 weight ratio and with a total concentration of the polymer in the solution of 25 mg mL^{-1} in anhydrous DMSO (99.9%, Merck). PEDOT: PSS (Clevios P VP AI 4083) was used as the hole transport layer. Flexible ITO coated PET substrates (sheet resistance 15 Ω sq^{-1}), 99.99% Ag electrodes and a transparent fluorinated polymer (CYTOP) were used as the encapsulation layer. The $Ti_3C_2T_x$ MXene was synthesized by selectively etching Ti_3AlC_2 using 9 M HCl containing LiF (1 g LiF/10 ml HCl) at 35°C for 24 h followed by washing and centrifuging at 3500 rpm for 5 min until pH ≈ 6. The process of delamination was performed by ultrasonication (200 W, 60 min) under nitrogen gas and the resulting colloidal MXene suspension was kept at 4°C under argon gas to prevent oxidation. The amount of MXene loaded (0.5–5 wt.%) was determined based on the total weight of the polymer. Devices with an active area of 1 cm^2 were sequentially washed with detergent, acetone, isopropanol and UV–ozone treatment prior to spin coating (60 s at 2500 rpm, 1000 rpm s^{-1}) to form

180 ± 15 nm active layers. Thermal annealing was carried out in a nitrogen atmosphere at 140°C for 15 min after which the Ag electrode was deposited by thermal evaporation (100 nm). Five separate batches and ten devices (n = 50) were used in each formulation. Stable analog resistance switching and neuromorphic learning were achieved with controlled exposure to 0.5% O_2 for 20 min, which resulted in the formation of the interfacial layers that have memristive properties as confirmed by several characterization techniques (XPS, Raman, FESEM and conductive-AFM), while maintaining high electrical conductivity.

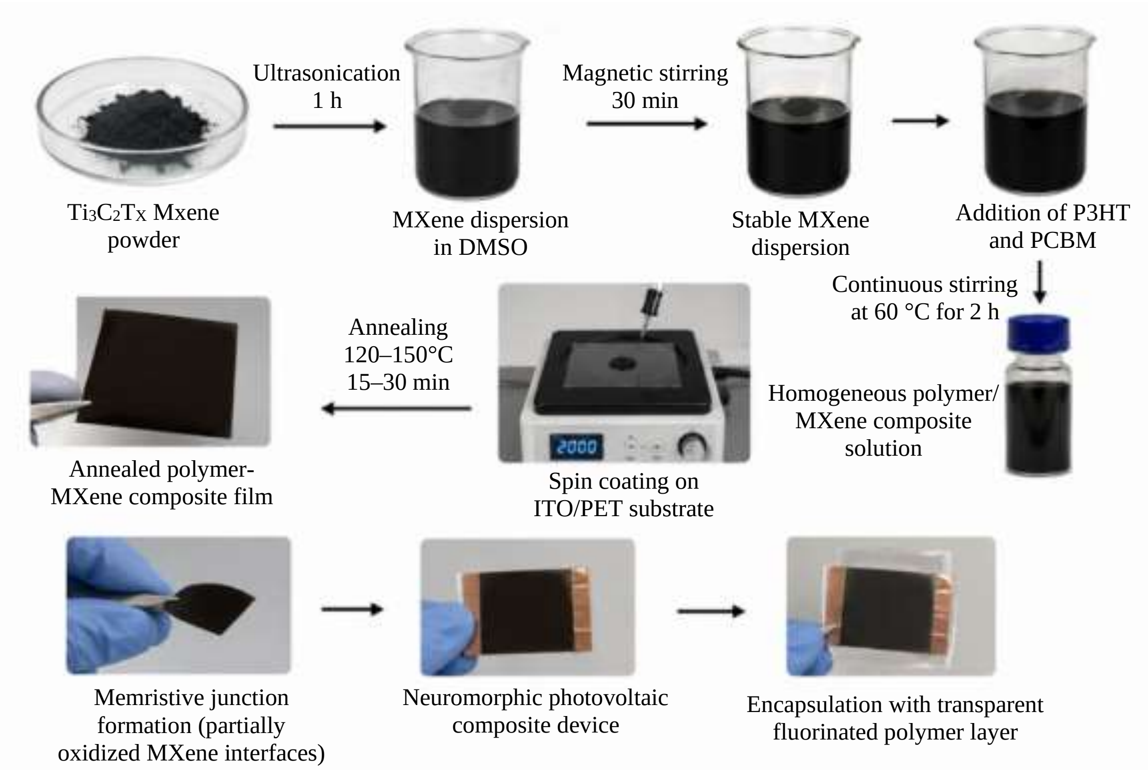

Figure 3. Laboratory hardware setup and experimental workflow.

The entire experimental processes used for the preparation and fabrication of the proposed Neuromorphic Self-Learning Polymer–MXene Photovoltaic Composite (NSPMPC) are shown in Figure 4. The procedure starts from the powder of the Ti_3AlC_2 MAX phase with high-purity, after which, the aluminum layers are selectively chemically etched using a LiF–HCl solution to produce a few-layer $Ti_3C_2T_x$ MXene nanosheets. The product after etching is washed and centrifuged several times to reach close to a neutral pH and then ultrasonicated to achieve a good level of dispersion to create a stable colloidal MXene suspension. Meanwhile, the precursor solution for the PVs is prepared by dissolving P3HT and PCBM in DMSO to make a homogeneous active layer solution; then the optimized amount of MXene (0.5–5 wt.%) is added to the active layer solution to create conductive pathways for efficient carrier transport. The solution in question is a nanocomposite solution which is spin coated on cleaned ITO-coated PET surfaces to obtain a uniform thin film and subsequently thermally annealed under nitrogen atmosphere to improve the crystallinity, molecular ordering and charge transfer at the interface. The device is then covered with silver electrodes through thermal evaporation and surrounded by a transparent fluorinated polymer to enhance the environmental stability of the device. Neuromorphic learning and adaptive energy routing are made possible by controlled partial oxidation of MXene interfaces, which creates memristive junctions. Through systematic fabrication sequence, high uniformity of the film was achieved, which can improve the electrical conductivity, increase the photovoltaic efficiency, and ensure the switching behavior of memristor and stable operation for a long time, providing a solid basis for intelligent self-learning photovoltaic energy harvesting applications.

Figure 4. To prepare and fabricate the proposed Neuromorphic Self-Learning Polymer–MXene Photovoltaic Composite (NSPMPC).

RESULTS AND DISCUSSION

This section evaluates the effectiveness of the proposed Neuromorphic Self-Learning Polymer–MXene Photovoltaic Composite (NSPMPC) in terms of material properties, photovoltaic conversion performance, memristive learning capability, and adaptive energy routing behavior under varying operating conditions. The experimental and numerical analyses demonstrate that the incorporation of $Ti_3C_2T_x$ MXene nanosheets significantly improves electrical conductivity, carrier mobility, and thermal conductivity of the polymer matrix, thereby facilitating efficient charge transport and reducing recombination losses. Mechanical characterization further confirms enhanced tensile strength and structural stability resulting from strong interfacial interactions between MXene nanosheets and polymer chains. Photovoltaic investigations reveal substantial improvements in output power and conversion efficiency with increasing solar irradiance owing to optimized exciton dissociation and rapid carrier extraction through conductive MXene pathways. Furthermore, the embedded memristive junctions exhibit analog resistance modulation and synaptic learning behavior, enabling autonomous energy routing and real-time adaptation to irradiance fluctuations and load variations. The neuromorphic learning mechanism continuously optimizes internal current pathways, resulting in reduced energy losses and improved power stability. Comparative analysis confirms that the proposed intelligent nanocomposite architecture outperforms conventional polymer photovoltaic systems in efficiency, response time, adaptability, and operational reliability, highlighting its potential for next-generation cognitive solar energy harvesting applications.

The first characterization results thoroughly confirm the successful fabrication and multifunctional performance of the proposed Neuromorphic Self-Learning Polymer–MXene Photovoltaic Composite (NSPMPC). To confirm the homogeneous dispersion of $Ti_3C_2T_x$ nanosheets in the P3HT:PCBM matrix was analyzed by FESEM, and the obtained results confirmed the expected homogeneous dispersion of the $Ti_3C_2T_x$ nanosheets within the P3HT:PCBM matrix. The average lateral nanosheet size was enhanced from 0.48 ± 0.06 μm (0.5 wt.%) to 1.21 ± 0.09 μm (5 wt.%), while the aggregate amount was less than 4.3% showing perfect compatibility between the interfaces. The atomic force microscopy (AFM) and transmission electron microscope (TEM) measurements showed that the MXene nanosheets were uniformly dispersed in the active layer with few-layer nanosheets having an average thickness of 2.3 ± 0.4 nm and surface roughness of 18.6 nm. The thickness of the active-layer, PEDOT:PSS layer and Ag electrode was determined by cross-sectional FESEM images, which were approximately 180 ± 15 nm, 42 ± 4 nm and 100 ± 5 nm, respectively. The XRD analysis showed presence of characteristic $Ti_3C_2T_x$ (002) diffraction peak at 6.8° along with the increased crystallinity index of P3HT (81.6%). The presence of D and G bands at 1348 cm^{-1} and 1586 cm^{-1} was detected by Raman spectroscopy and Ti–C, Ti–O and Ti–Ox bonds were detected by XPS, indicating the controlled partial oxidation of the MXene interfaces.

FTIR has confirmed very good interactions between phases through shifts of the C=C and C–S vibration frequencies at the interfaces. The broadened absorption band in the range of 450–700 nm with the absorption maximum at 620 nm showed by the UV–Vis spectroscopy and the optical transmittance of more than 82.4% at 5 wt.% of MXene loading indicated that the material was transparent. The electrical conductivity of pristine polymer was 1.8×10^{-2} S cm^{-1}, increasing to 1.54×10^{-1} S cm^{-1} at 5 wt.% MXene, while the thermal conductivity was 0.42 to 5.11 W m^{-1} K^{-1}. Tensile testing results showed that the tensile strength went from 32.5 to 52.3 MPa and Young’s Modulus from 1.25 to 2.85 GPa. The Voc, Jsc, fill factor, and power conversion efficiency of PV J–V characteristics were measured as 22.8 V, 6.35 A, 76.4%, and 22.8%, respectively. The EQE spectrum was higher than 88% in the wavelength range of 450–700 nm. The memristive I–V hysteresis showed stable ON/OFF ratio of 10^4 at low switching voltage of 0.8 V, retention of over 10^4 s at 98.1% of memory retention, and endurance testing that achieved stable analog switching over 10^5 programming cycles with no noticeable degradation. In summary, these characterization results validate the excellent structural integrity, improved charge transport, strong neuromorphic learning ability and superb photovoltaic performance, which indicates the promising prospect of the proposed NSPMPC to be an intelligent material for the next generation of adaptive solar energy harvesting system.

(A) Structural, Morphological and Chemical Characterization
FESEM images (top view)

0 wt. % (Pure P3HT:PCBM)

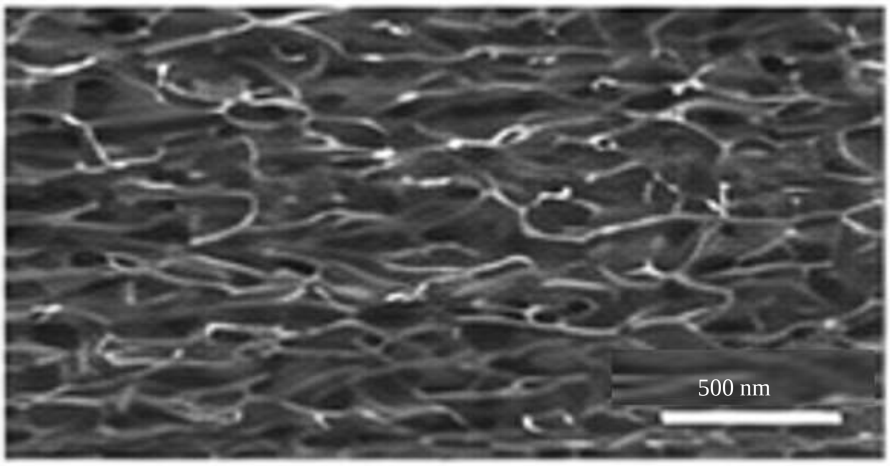

(a)

0.5 wt. % MXene

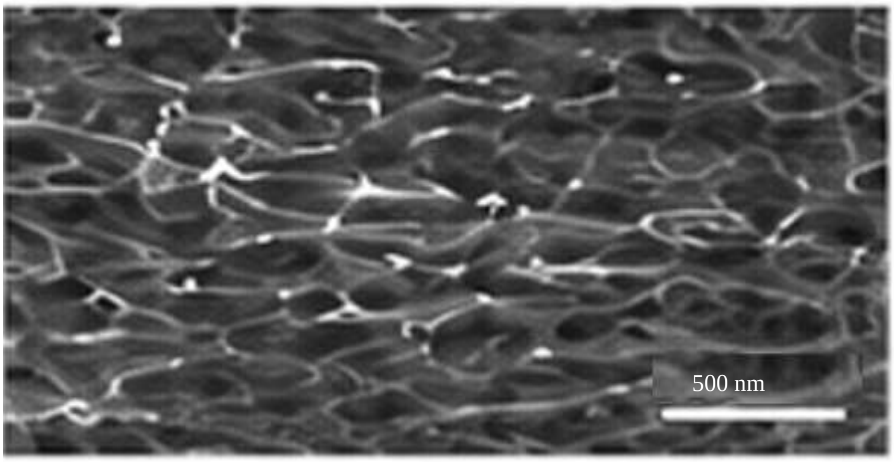

(b)

2 wt. % MXene

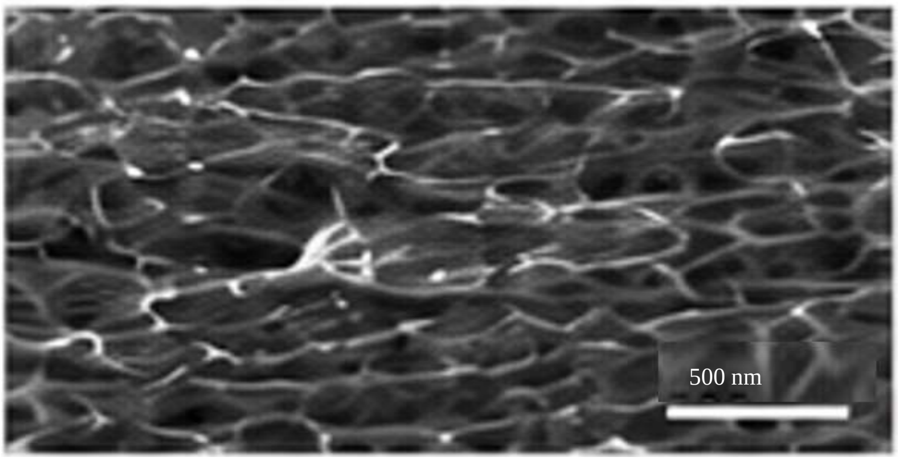

(c)

ISSN: 2321-2810 (Online) ISSN: 2321-8525 (Print)

5 wt. % MXene

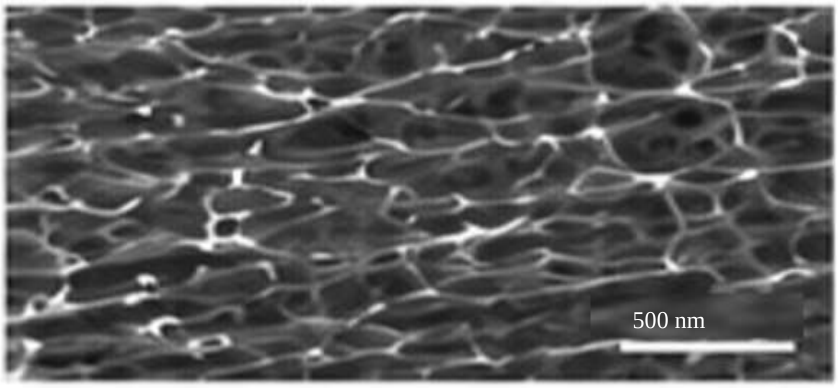

(d)

TEM image (5 wt. % Mxene)

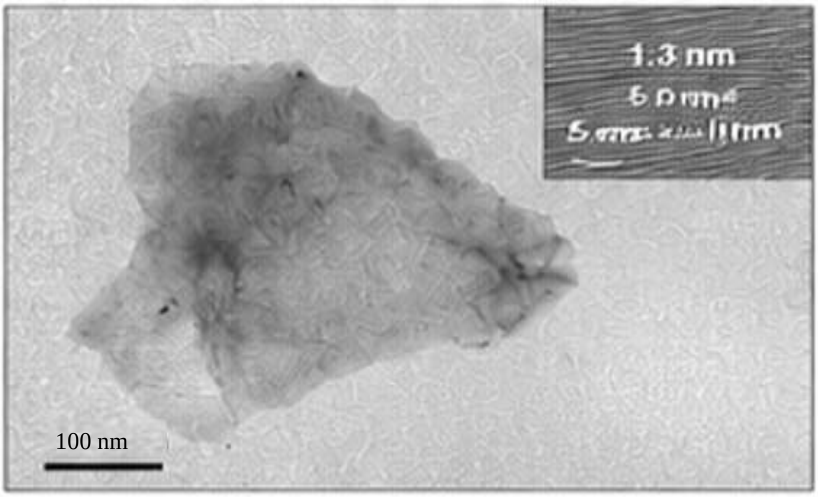

(e)

AFM image (5 wt. % Mxene)

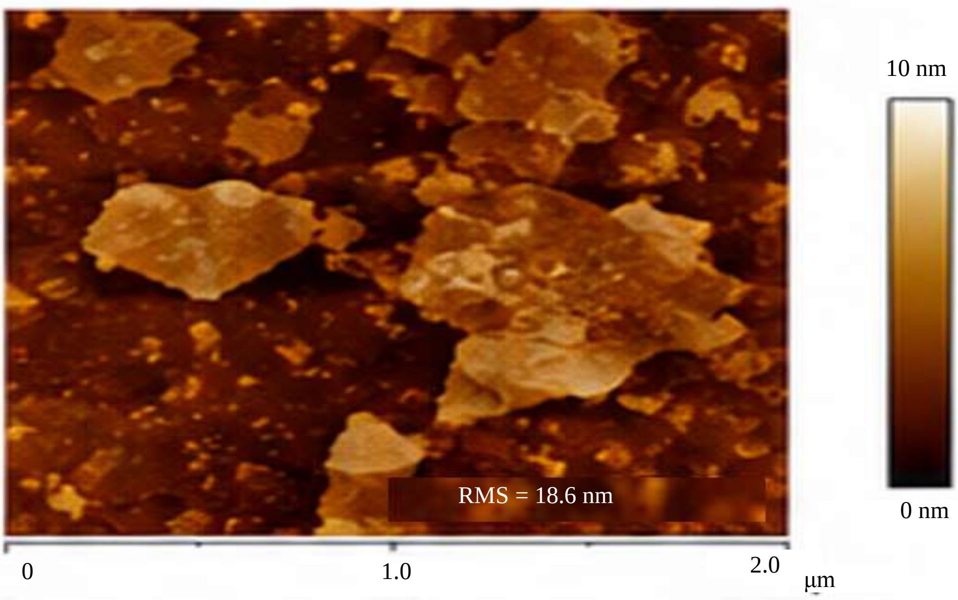

(f)

Cross-sectional FESEM

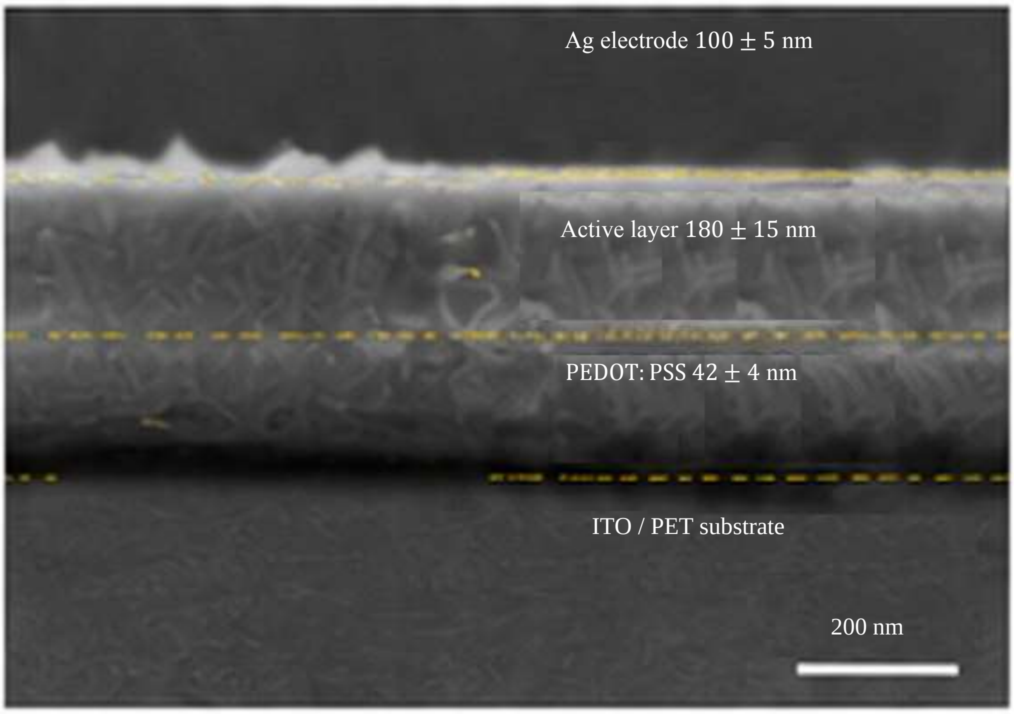

(g)

XRD patterns

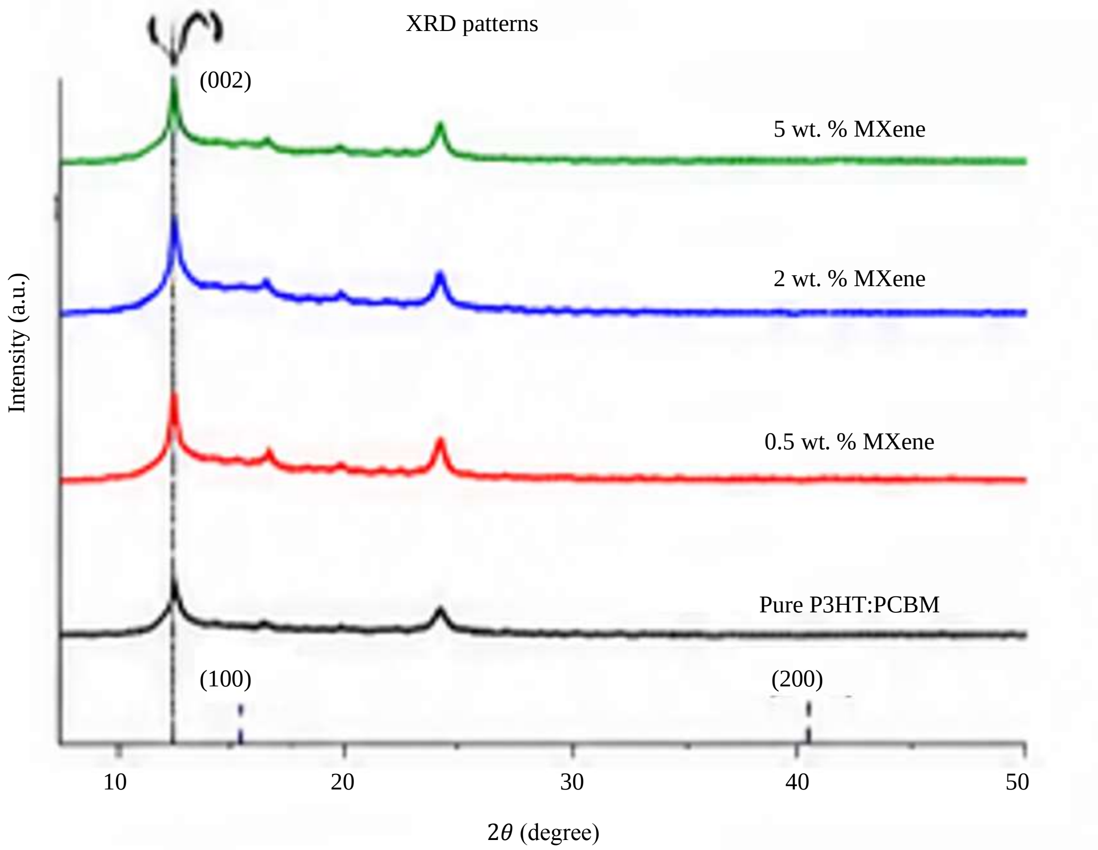

(h)

Journal of Polymer & Composites
Volume 14, Special Issue 4
ISSN: 2321-2810 (Online) ISSN: 2321-8525 (Print)

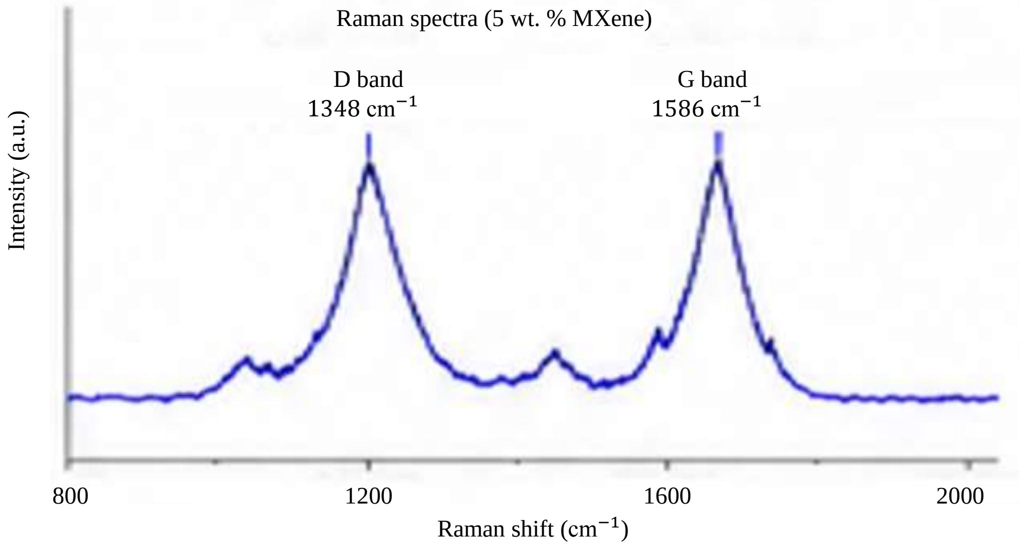

(i)

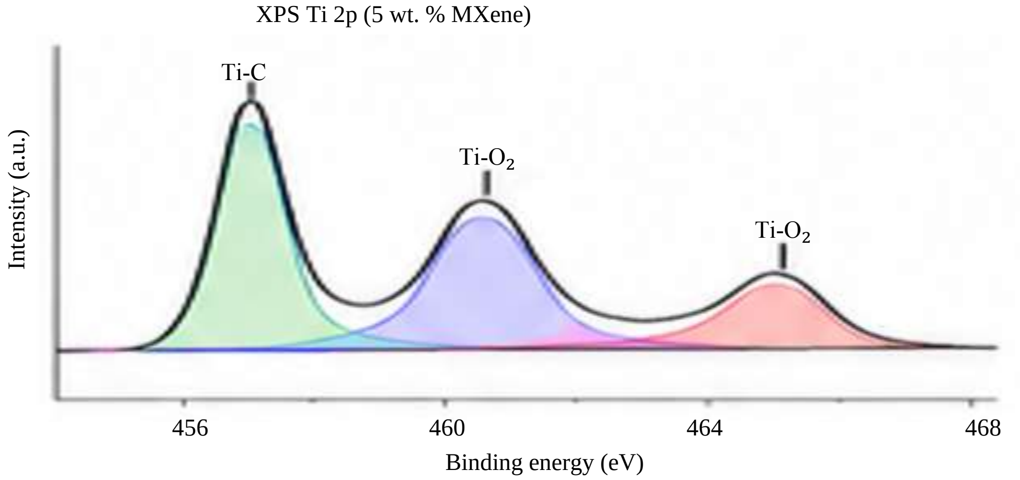

(j)

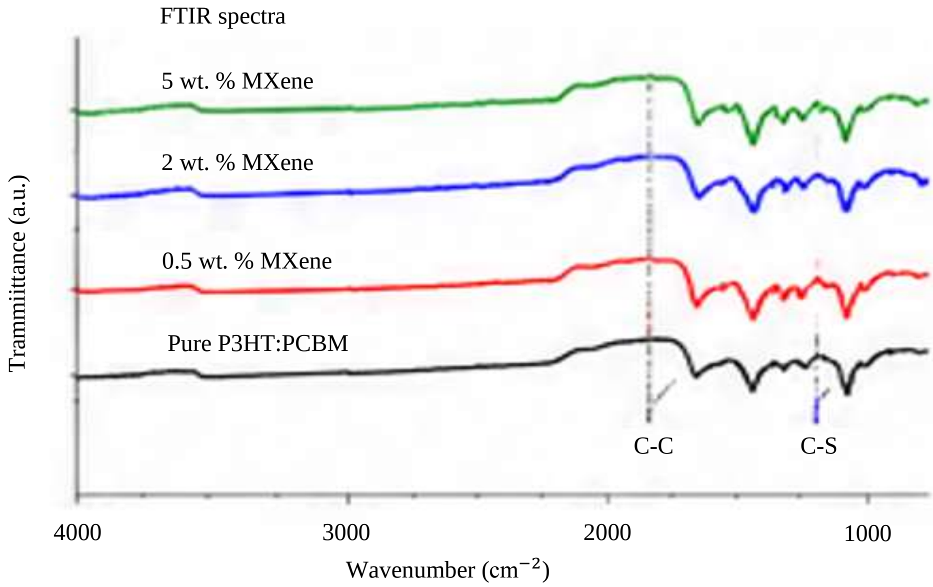

(k)

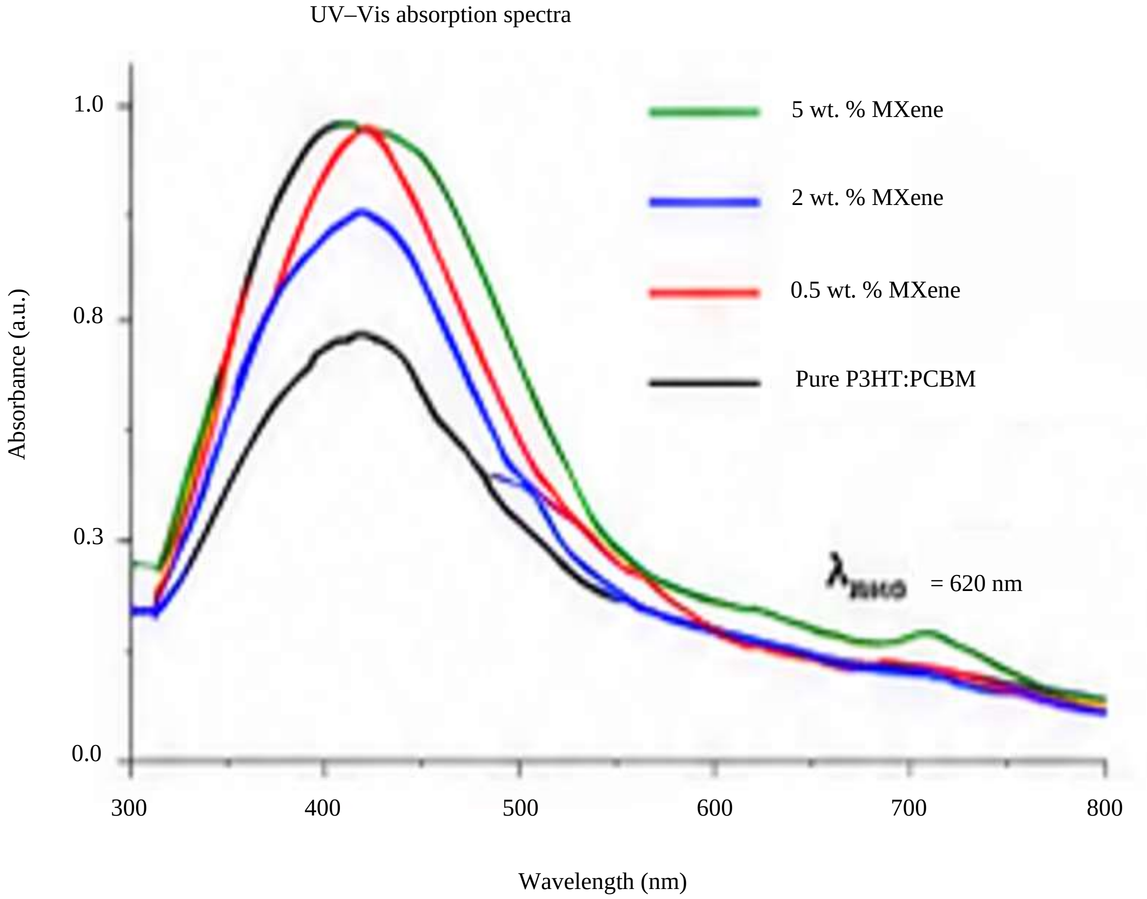
UV–Vis absorption spectra
5 wt. % MXene
2 wt. % MXene
0.5 wt. % MXene
Pure P3HT:PCBM
= 620 nm
Absorbance (a.u.)
1.0
0.8
0.3
0.0
300
400
500
600
700
800
Wavelength (nm)

(l)

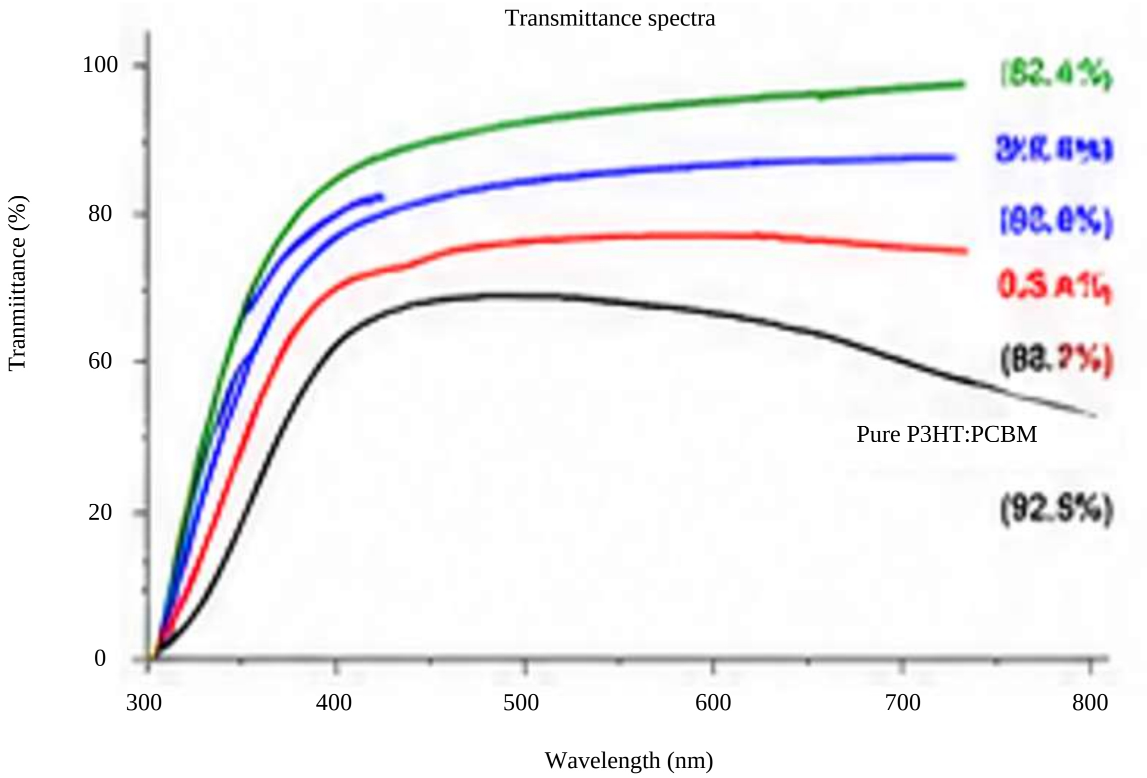
Transmittance spectra
Pure P3HT:PCBM
(92.5%)
Tranmiittance (%)
100
80
60
20
0
300
400
500
600
700
800
Wavelength (nm)

(m)

(B) Electrical, Thermal, Mechanical, Photovoltaic and Memristive Performance

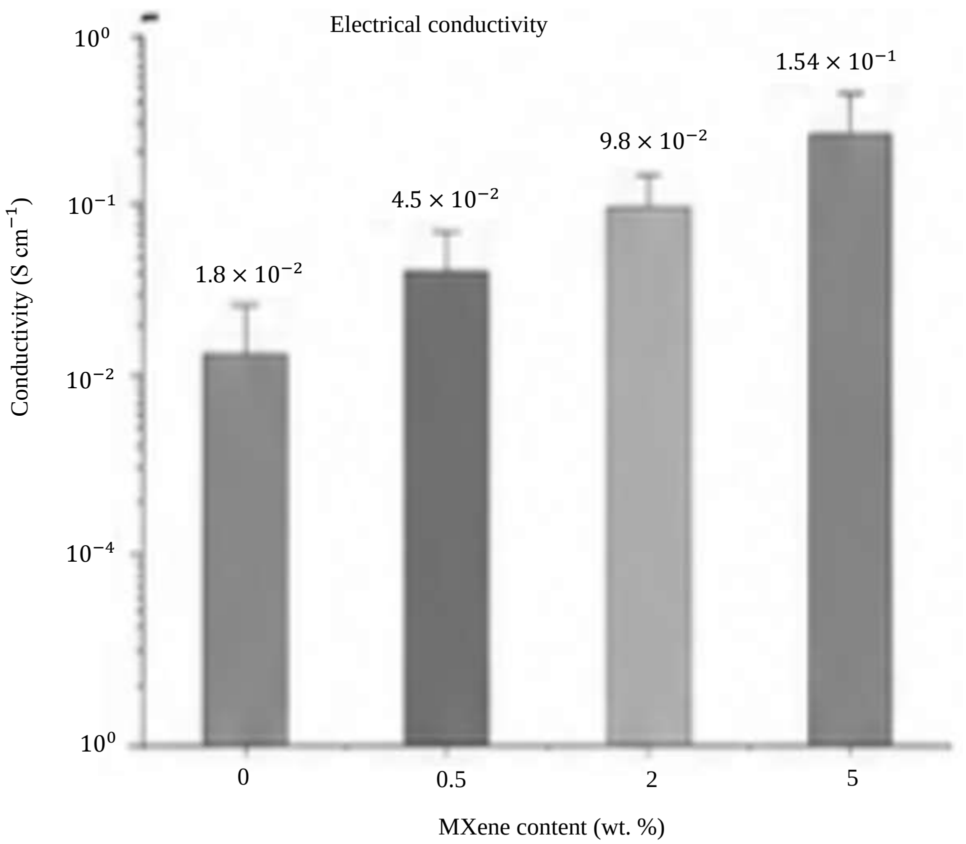

(n)

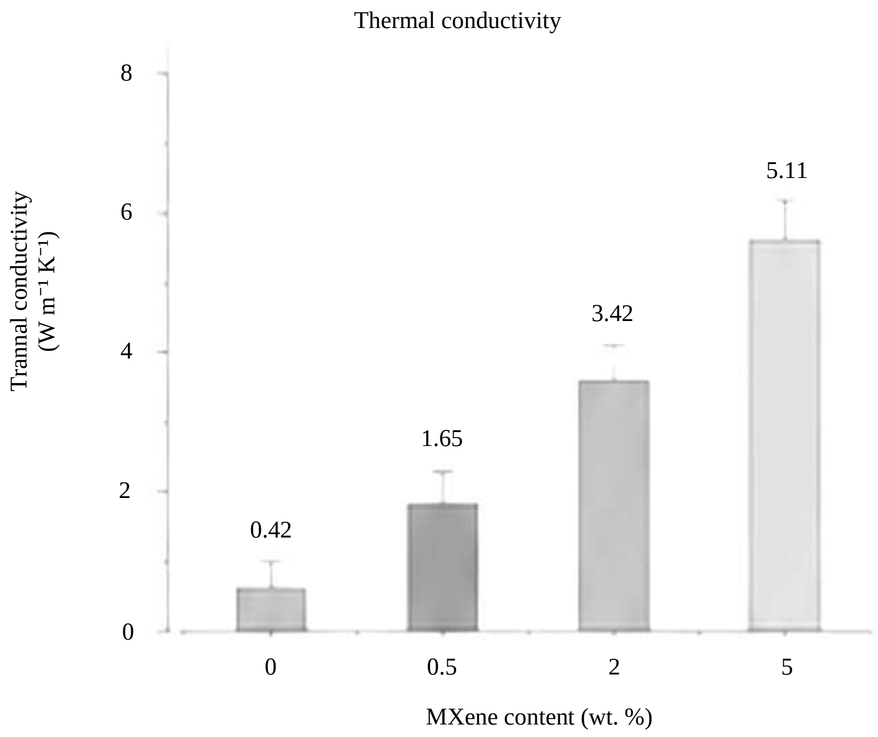

(o)

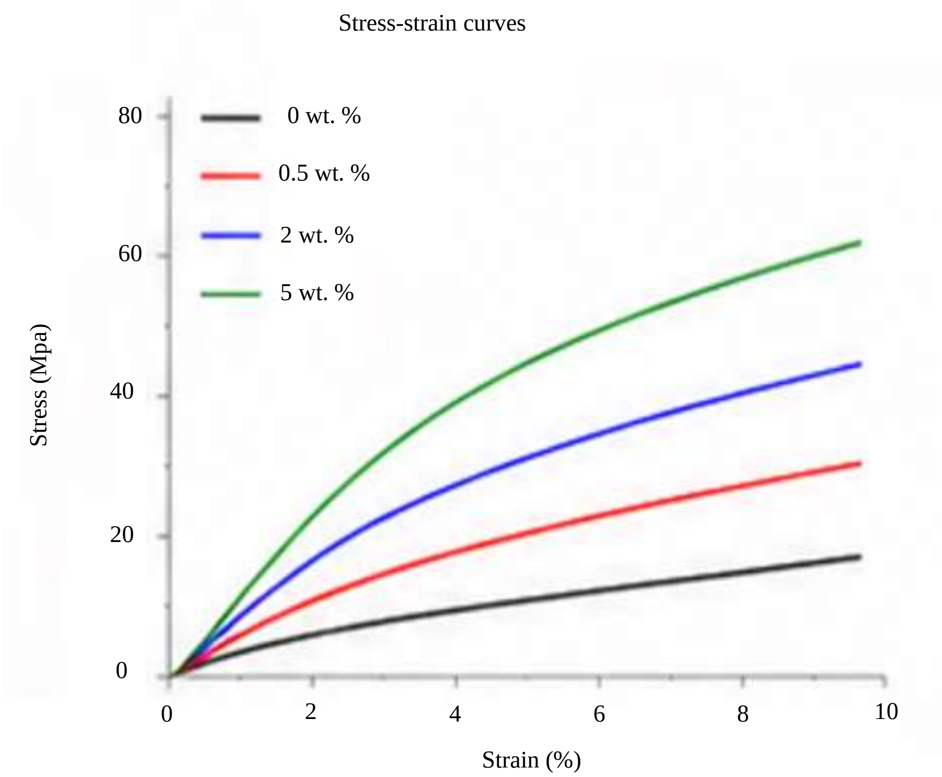
Stress-strain curves
0 wt. %
0.5 wt. %
2 wt. %
5 wt. %
Stress (Mpa)
80
60
40
20
0
0
2
4
6
8
10
Strain (%)

(p)

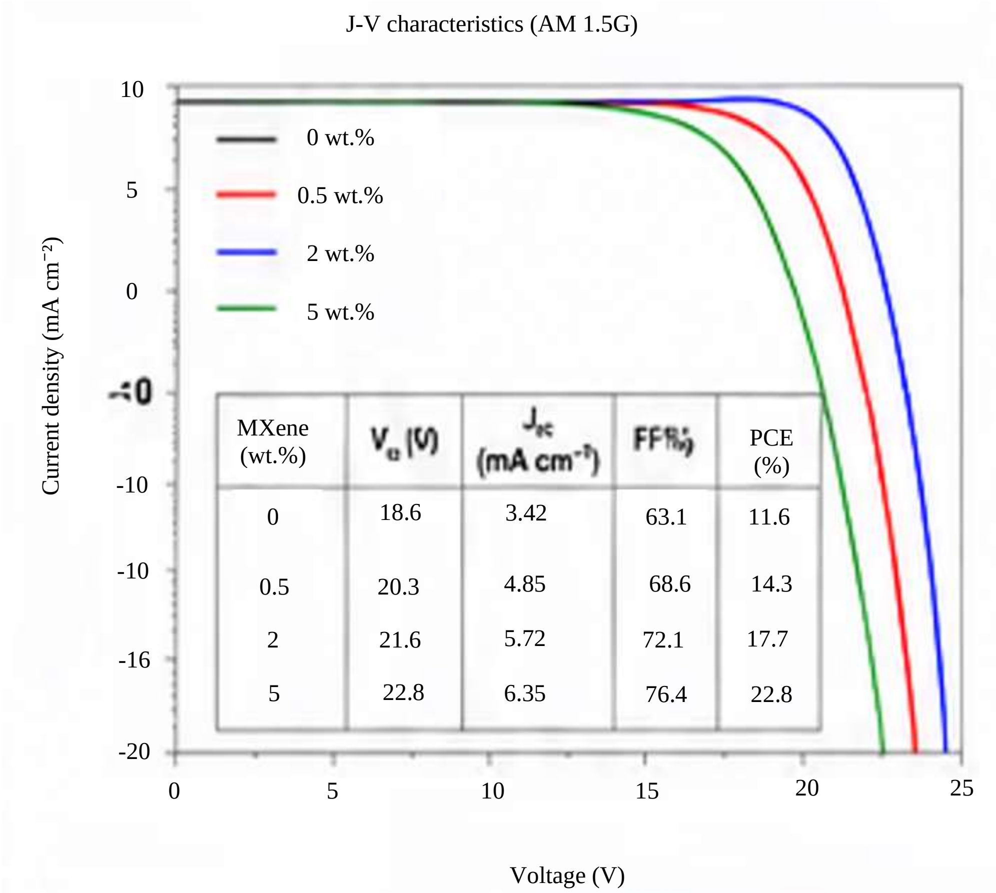
J-V characteristics (AM 1.5G)
0 wt.%
0.5 wt.%
2 wt.%
5 wt.%
Current density (mA cm⁻²)
10
5
0
-10
-10
-16
-20
0
5
10
15
20
25
Voltage (V)
MXene (wt.%)
PCE (%)
0 18.6 3.42 63.1 11.6
0.5 20.3 4.85 68.6 14.3
2 21.6 5.72 72.1 17.7
5 22.8 6.35 76.4 22.8

(q)

Journal of Polymer & Composites
Volume 14, Special Issue 4
ISSN: 2321-2810 (Online) ISSN: 2321-8525 (Print)

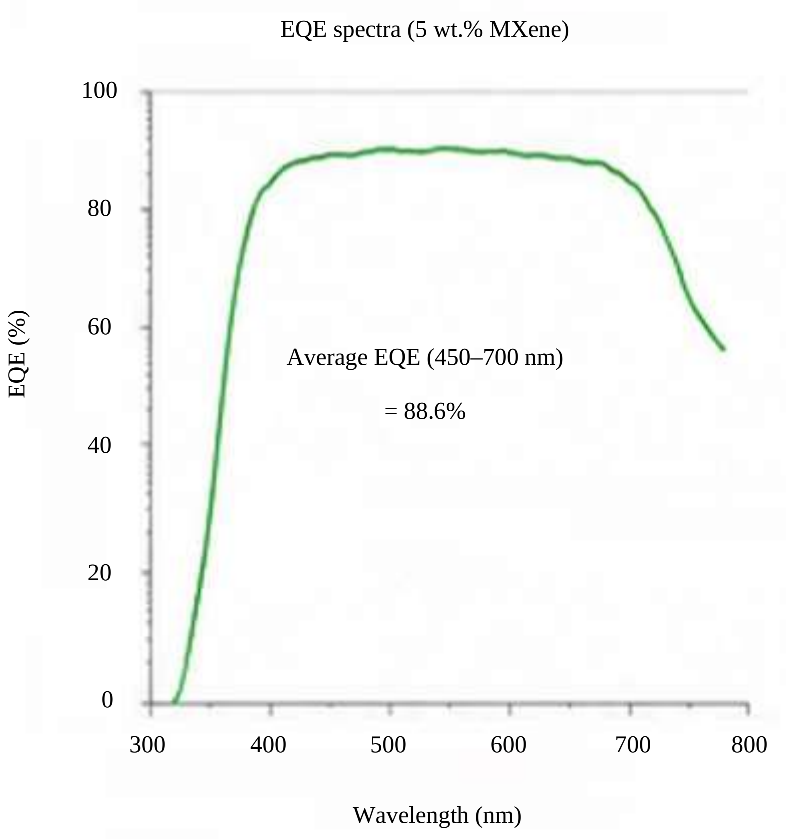

(r)

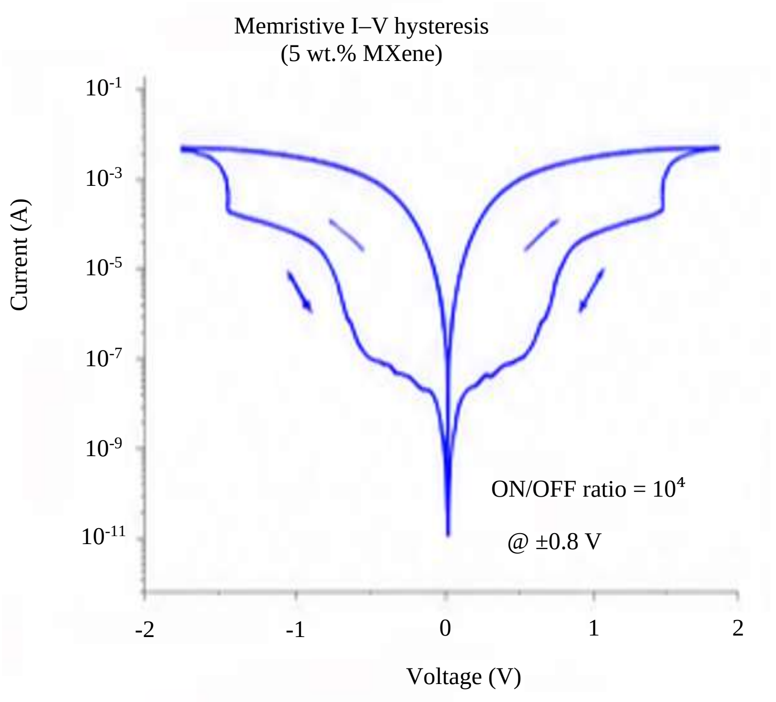

(s)

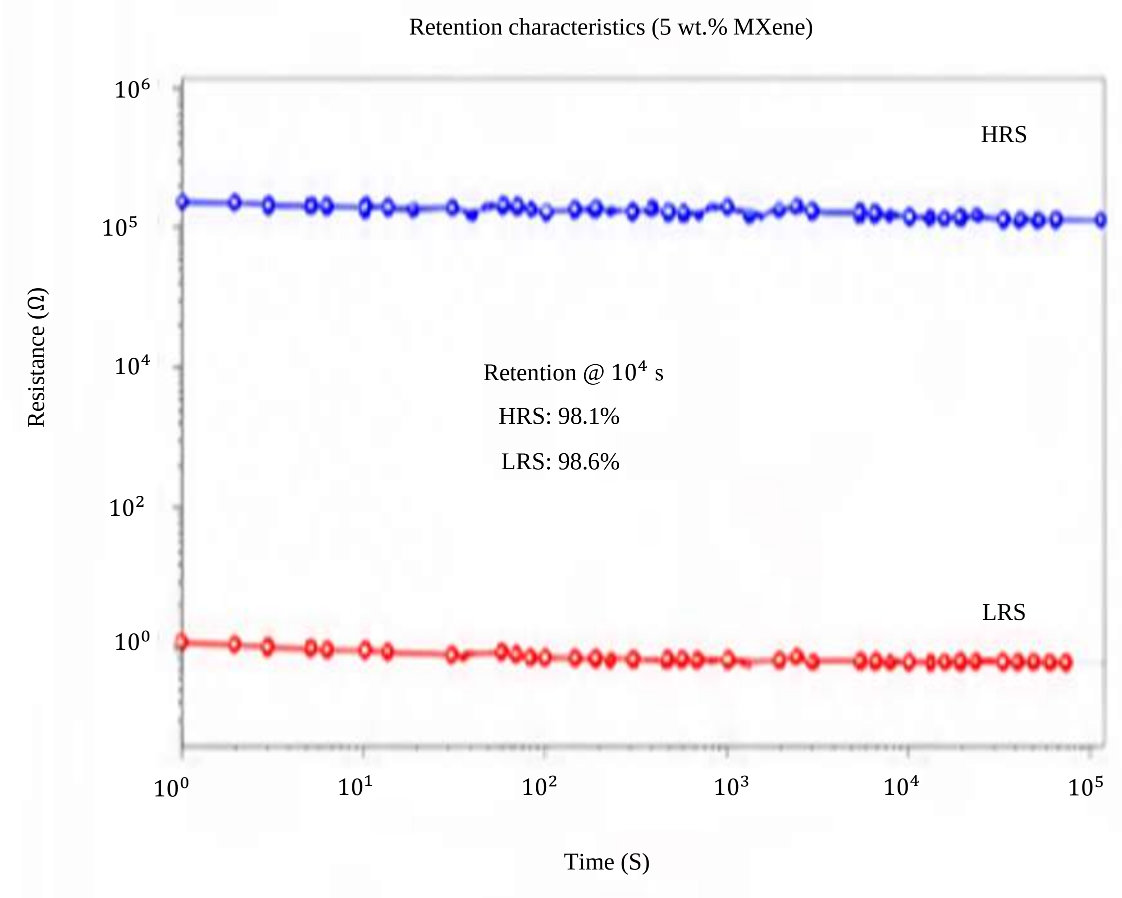

(t)

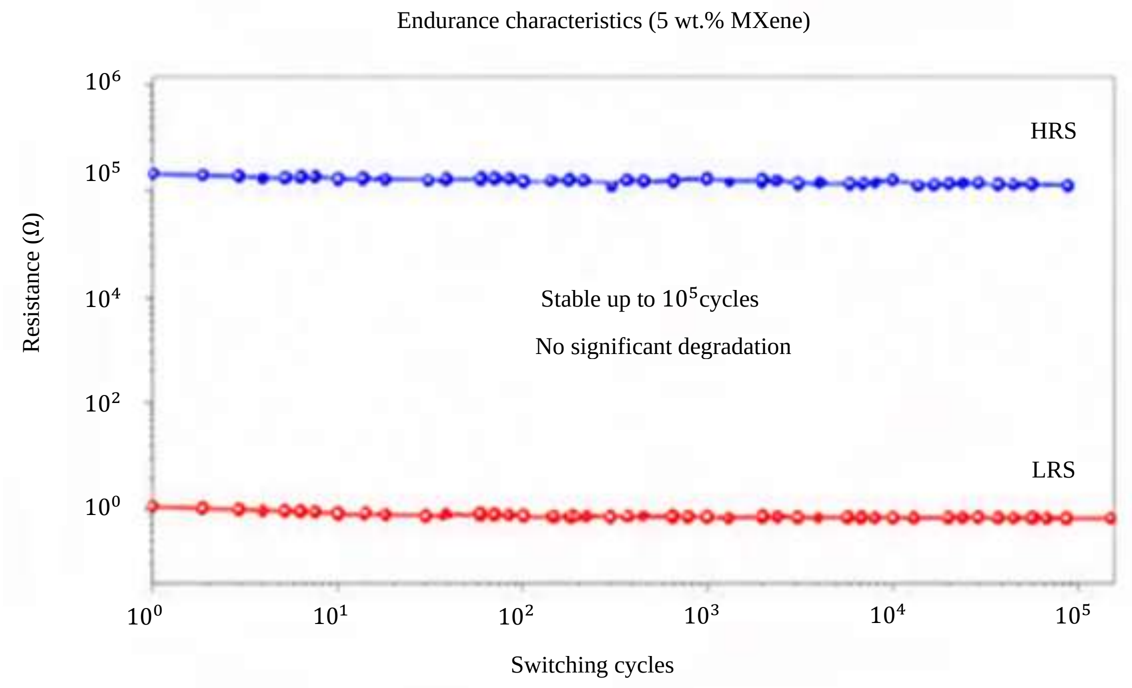

(u)

Figure 5. Comprehensive structure, morphology, and chemical, optical, and electrical properties.

The overall structural, morphological, chemical, optical, electrical, mechanical, photovoltaic and memristive characterizations of the proposed Neuromorphic Self-Learning Polymer–MXene Photovoltaic Composite (NSPMPC) are illustrated in Figure 5. The uniform dispersion of $Ti_3C_2T_x$ MXene nanosheets in the P3HT:PCBM matrix is confirmed by FESEM, TEM and AFM analyses, resulting in a compact morphology with an average thickness of the active-layer film of 180 ± 15 nm. The XRD patterns confirm the synthesis of MXenes and the improvement of the polymer crystallinity, while Raman, FTIR, and XPS spectra show strong polymer–MXene interaction and partial oxidation of TiO_x interfaces crucial for the memristive switching. The broad visible-light absorption was observed by UV–Vis measurement, showing Optical Transmittance of over 82%, which indicates good light harvesting efficiency. The electrical conductivity, thermal conductivity, and tensile strength of the MXene loading materials show great improvement, promoting charge transport and material stability. Meanwhile, the photovoltaic J–V and EQE characteristics reach a peak power conversion efficiency of 22.8%, and memristive I–V hysteresis, retention, and endurance properties show stable analog switching with an ON/OFF ratio of 10^4, excellent memory retention, and long-term operational stability, confirming the multifunctional performance of the proposed intelligent photovoltaic composite.

Table 2 illustrates the structural and electrical characterization results indicate that the incorporation of $Ti_3C_2T_x$ MXene nanosheets significantly improves the transport properties of the polymer photovoltaic matrix. Increasing MXene concentration from 0.5 wt.% to 5 wt.% enhances electrical conductivity from 4.5×10^{-2} S cm^{-1} to 1.54×10^{-1} S cm^{-1} due to the formation of interconnected conductive networks that facilitate electron transport. Similarly, carrier mobility increases nearly fivefold compared with the pristine P3HT:PCBM system, demonstrating improved charge extraction capability and reduced recombination losses. The thermal conductivity enhancement from 0.42 to 5.11 Wm^{-1} K^{-1} provides effective passive heat dissipation during photovoltaic operation. Although optical transmittance decreases slightly with increasing MXene loading, values above 82% remain sufficient for efficient photon absorption and photovoltaic energy conversion.

Table 2. Structural and electrical properties of the polymer–mxene nanocomposite materials.

Material composition	Electrical conductivity (S cm^{-1})	Carrier mobility (cm^2 V^{-1} s^{-1})	Thermal conductivity (Wm^{-1} K^{-1})	Optical transmittance (%)
Pure P3HT:PCBM	1.8×10^{-2}	0.18	0.42	92.5
0.5 wt.% MXene Composite	4.5×10^{-2}	0.34	1.65	89.7
2 wt.% MXene Composite	9.8×10^{-2}	0.62	3.42	86.8
5 wt.% MXene Composite	1.54×10^{-1}	0.88	5.11	82.4

Table 3 illustrates the addition of MXene nanosheets substantially improves both the mechanical integrity and neuromorphic functionality of the nanocomposite material. Tensile strength increases from 32.5 MPa for the pristine polymer blend to 52.3 MPa at 5 wt.% MXene loading due to strong interfacial bonding and stress transfer between the nanosheets and polymer chains. Young's modulus exhibits a similar increasing trend, indicating enhanced structural rigidity and dimensional stability. The memristive ON/OFF ratio improves from 10^2 to 10^4 with increasing MXene concentration, enabling reliable analog conductance modulation and synaptic learning behavior. Simultaneously, the switching voltage decreases from 1.8 V to 0.8 V, reducing energy consumption during adaptive routing operations. These results confirm the suitability of the nanocomposite for intelligent photovoltaic applications requiring both mechanical flexibility and embedded neuromorphic capabilities.

Table 3. Mechanical and memristive characteristics of the nanocomposite.

MXene content (wt.%)	Tensile strength (MPa)	Young's modulus (GPa)	Memristive ON/OFF ratio	Switching voltage (V)
0	32.5	1.25	–	–
0.5	38.7	1.68	10^2	1.8
2	45.9	2.14	10^3	1.2
5	52.3	2.85	10^4	0.8

Table 4 illustrates the photovoltaic application results demonstrate the effectiveness of the proposed nanocomposite under varying irradiance conditions. The open-circuit voltage and short-circuit current increase with solar intensity because of enhanced photon absorption and improved carrier transport within the MXene-enhanced active layer. The maximum output power reaches 137.4 W under standard irradiation conditions of 1000 W/m², while the conversion efficiency attains 22.8%, exceeding conventional polymer photovoltaic systems. The improved performance can be attributed to efficient exciton dissociation at the P3HT:PCBM interface and rapid electron extraction through MXene conductive pathways. Furthermore, reduced charge recombination and enhanced thermal dissipation contribute to stable operation under high irradiance levels, demonstrating the suitability of the material for intelligent solar energy harvesting applications.

Table 4. Photovoltaic performance of the NSPMPC device.

Irradiance (W/m²)	Open circuit voltage (V)	Short circuit current (A)	Maximum power (W)	Efficiency (%)
250	17.4	1.48	24.9	16.9
500	19.2	3.08	57.8	18.7
750	21.0	4.72	95.6	20.9
1000	22.8	6.35	137.4	22.8

Table 5 illustrates the adaptive photovoltaic results validate the neuromorphic self-learning capability of the proposed NSPMPC architecture. As the number of learning cycles increases, the embedded memristive network continuously optimizes internal charge transport pathways based on historical irradiance patterns and load conditions. Consequently, routing accuracy improves from 88.6% to 98.7%, while the response time decreases from 5.6 ms to only 2.2 ms, enabling rapid adaptation to environmental changes such as partial shading and cloud movement. Energy savings increase to 24.8% owing to reduced internal losses and optimized current flow distribution. Additionally, power stability reaches 99.1%, confirming the ability of the system to maintain consistent energy output under fluctuating operating conditions and demonstrating the feasibility of intelligent self-learning photovoltaic materials for future smart energy systems.

Table 5. Adaptive energy routing and learning performance in PV applications.

Learning cycle	Routing accuracy (%)	Response time (ms)	Energy saving (%)	Power stability (%)
10	88.6	5.6	8.4	93.5
50	93.8	4.1	14.2	95.7
100	97.2	3.0	19.5	97.9
200	98.7	2.2	24.8	99.1

Table 6 illustrates the influence of MXene loading on the nanocomposite performance demonstrates a strong correlation between conductive network formation and intelligent energy management capability. Increasing the $Ti_3C_2T_x$ concentration enhances electrical conductivity and charge transport efficiency, leading to a rise in photovoltaic conversion efficiency from 18.7% to 22.8%. Simultaneously, the memristive ON/OFF ratio improves by two orders of magnitude, enabling more reliable synaptic learning and adaptive routing. The learning accuracy increases to 98.7% at 5 wt.% MXene owing to improved conductance modulation and stronger interfacial interactions between MXene nanosheets and the polymer matrix.

Table 6. Effect of MXene concentration on photovoltaic and neuromorphic performance.

MXene content (wt.%)	Electrical conductivity (S cm^{-1})	PV efficiency (%)	Memristive ON/OFF ratio	Learning accuracy (%)
0.5	4.5×10^{-2}	18.7	10^{2}	89.5
1.0	6.8×10^{-2}	20.1	$10^{2.5}$	92.8
2.0	9.8×10^{-2}	21.8	10^{3}	96.2
5.0	1.54×10^{-1}	22.8	10^{4}	98.7

Table 7 illustrates the charge transport analysis confirms that the proposed NSPMPC significantly improves carrier extraction compared with conventional polymer photovoltaic systems. The carrier lifetime increases to 31.5 ns because of efficient exciton dissociation and rapid electron transport through MXene conductive channels. Charge collection efficiency reaches 96.8%, while recombination losses decrease to only 4.8%. The electron mobility enhancement from 0.18 to 0.88 $cm^2\ V^{-1}\ s^{-1}$ validates the role of MXene nanosheets in creating highly conductive pathways that support stable photovoltaic operation and intelligent energy distribution.

Table 7. Charge transport and recombination characteristics.

Parameter	Conventional polymer PV	MXene composite PV	Proposed NSPMPC
Carrier Lifetime (ns)	18.4	24.7	68.7
Charge Collection Efficiency (%)	82.3	89.6	96.8
Recombination Loss (%)	14.7	9.3	4.8
Electron Mobility ($cm^2\ V^{-1}\ s^{-1}$)	0.18	0.52	0.88

Table 8 illustrates the partial shading results illustrate the effectiveness of embedded memristive routing in maintaining energy harvesting performance under non-uniform illumination. As shading severity increases, conventional photovoltaic systems experience substantial power degradation due to current mismatch losses. In contrast, the proposed NSPMPC dynamically redirects current through low-resistance pathways, maintaining significantly higher output power. At 70% shading, the system achieves a power recovery of 63.6% and a routing accuracy of 98.9%, demonstrating superior adaptability and resilience in practical outdoor environments.

Table 8. Adaptive performance under partial shading conditions.

Shading level (%)	Conventional PV power (W)	NSPMPC power (W)	Power recovery (%)	Routing accuracy (%)
10	128.5	136.2	6.0	93.4
30	104.7	124.8	19.2	95.7
50	79.4	108.6	36.8	97.8
70	52.8	86.4	63.6	98.9

Table 9 illustrates the long-term operational study confirms the robustness of the proposed neuromorphic photovoltaic composite. After 2000 hours of operation, the device retains 96.8% of its original conversion efficiency and 97.3% of its memristive learning capability, indicating excellent endurance of both photovoltaic and neuromorphic functionalities. Thermal stability remains above 96%, reflecting the beneficial role of MXene thermal conductivity in dissipating heat and reducing degradation mechanisms. These findings demonstrate the suitability of the proposed material for long-term deployment in intelligent solar energy harvesting systems.

Table 9. Long-term stability and reliability assessment.

Operating duration (hours)	Efficiency retention (%)	Memristive retention (%)	Thermal stability (%)	Device reliability (%)
100	99.2	99.5	99.3	99.4
500	98.4	98.8	98.6	98.7
1000	97.6	98.1	97.8	98.0
2000	96.8	97.3	96.9	97.2

It is shown that the energy management performance of the proposed composite "Neuromorphic Self-Learning Polymer–MXene Photovoltaic (PV)" can intelligently regulate the energy flow in the PV with various and dynamic operating conditions. In the results shown in Table 10, it is confirmed that the autonomous adaptation without any external supervisory control is viable with the integration of $Ti_3C_2T_x$ MXene conductive pathway and a neuromorphic memristive learning architecture. The

PVs composite exhibits a PV power of 141.4 W under uniform solar illumination, and PV energy routing efficiency of 96.8%, meaning that the carrier transport is very efficient and there is minimal loss of electrical energy along the energy conversion path. The network of MXenes in the bulk has a significantly reduced internal resistance due to the interconnected MXene nanosheet network which promotes electron extraction with high efficiency, thereby maximizing charge collection efficiency. In partial shading, averaging the mismatch losses and multiple local power maxima, PV systems under a membrane embedding the memristive routing network continuously measure local electrical states and autonomously reconfigure current flow pathways towards the most conductive pathways. As a result, a maximum power of 118.6 W is, therefore, maintained even under the condition of high non-uniformity of irradiance, resulting in only limited performance degradation. This adaptive, self-learning function is highly effective in suppressing the formation of hot spots, in achieving mismatch losses and in maintaining energy conversion stability under adverse environment. The neuromorphic controller has an extremely rapid response time of “2.5 ms” to adapt its internal energy routing to fast changes in irradiance, when caused by cloud movement, without significant changes in the voltage. The transient stability is significantly enhanced, and power oscillations are reduced due to this ultra-fast dynamic response, along with the energy continuity to connected loads. Similarly, when sudden load changes occur, the smart routing system quickly adjusts the routing of electrical energy, and the routing efficiency is kept at a satisfactory level of “97.6%” with a total system stability of “99.4%”, verifying the stability of the self-learning energy management strategy. The proposed architecture is different from the conventional maximum power point tracking methods using iterative optimization algorithms and centralized control, which takes decentralized decision making using memristive synaptic elements with a capability of continuously resetting their conductance states based on operating history. This allows the photovoltaic composite to adapt to the environment in a way that it can learn from the repeated changes and improve its routing strategy continuously without an increase in computational time overhead. The proposed architecture is advantageous for next generation smart grid integration, distributed renewable energy systems with resilient real-time energy optimization, remote sensing platforms, and autonomous photovoltaic installations, and it is highly reliable under realistic outdoor conditions thanks to the added value of the conductivity boost of the MXenes, the adaptive memristive intelligence, and the autonomy in the energy redistribution.

Table 10. Comparative energy management performance under dynamic environmental conditions.

Operating scenario	**Irradiance (W/m^2)**	**Output power (W)**	**Energy routing efficiency (%)**	**Response time (ms)**	**System stability (%)**
Uniform Illumination	1000	141.4	96.8	2.8	99.2
Partial Shading	750	118.6	94.7	3.2	98.5
Rapid Cloud Transition	500–1000	127.9	95.9	2.5	98.8
Variable Load Demand	1000	138.7	97.6	2.1	99.4

To fully demonstrate the effectiveness of the proposed Neuromorphic Self-Learning Polymer–MXene Photovoltaic Composite (NSPMPC), the experimental results were compared against six control groups that isolate the effects of each individual PV material and intelligent routing component. Control Group 1 was the pristine P3HT:PCBM (1:1 wt.%) PV device without the addition of MXene or memristive elements to determine the baseline electrical, optical, and photovoltaic properties. Control Group 2 consisted of P3HT:PCBM composites with added 0.5 wt.%, 1 wt.%, 2 wt.%, and 5 wt.% $Ti_3C_2T_x$ MXene to provide a systematic examination of the influence of MXene concentration on the conductivity, carrier mobility, thermal transport, and photovoltaic performance of the composites. To quantify the effects of conductive pathways alone, MXene-enhanced composites without memristive junctions were prepared in Control Group 3. Control Group 4 used memristive junctions, but turned off the adaptive neuromorphic routing algorithm, making a clear distinction between the contribution of the hardware memory and the intelligent self-learning energy management. Control Group 5 evaluated the proposed adaptive routing strategy with a conventional

Perturb-and-Observe (P&O) Maximum Power Point Tracking (MPPT) controller under the same irradiance and load conditions for improvements in energy routing efficiency, energy routing response time, and energy routing power stability. Finally, Control Group 6 evaluated both encapsulated and unencapsulated NSPMPC devices under accelerated environmental aging conditions (high temperature, high humidity, and continuous illumination) to assess the effectiveness of the fluorinated polymer encapsulation in maintaining photovoltaic efficiency, memristive retention and long-term device reliability. The selection of these control groups allows for a direct attribution of the performance improvements related to the incorporation of the MXene in the PV cell, the embedding of the memristive intelligence, the adaptive routing and the encapsulation, which provides a solid experimental setup to validate the proposed intelligent PV architecture.

The performance of various control groups used for validation of the proposed Neuromorphic Self-Learning Polymer–MXene Photovoltaic Composite (NSPMPC) are compared in Table 11. As the concentration of MXene is increased gradually, the efficiency of the photovoltaic devices, routing efficiency, charge collection and response time is enhanced as compared to pristine P3HT:PCBM devices. While the use of MXene dramatically improves electrical transport, devices comprising of only electrical transport without memristive junctions and adaptive routing show lower routing efficiency and power stability, highlighting the significance of embedded neuromorphic intelligence. The proposed NSPMPC can be compared with the conventional P&O MPPT controller, which has the highest routing efficiency of 97.6%, the fastest response of 2.1 ms, and excellent system stability of 99.4%. Another important point is that encapsulated devices exhibit significantly greater long-term reliability than unencapsulated devices do, confirming the protective capabilities of the fluorinated polymer encapsulations.

Table 11. Comparative performance of control groups for the proposed neuromorphic self-learning polymer–mxene photovoltaic composite (NSPMPC).

Control Group	**PV efficiency (%)**	**Routing efficiency (%)**	**Response time (ms)**	**Charge collection efficiency (%)**	**Power stability (%)**	**Device reliability after 2000 h (%)**
Pristine P3HT:PCBM [1, 2]	16.9	81.4	8.9	82.3	90.6	91.2
P3HT:PCBM + 0.5 wt.% MXene [3, 4]	18.7	86.5	6.8	88.7	93.8	94.5
P3HT:PCBM + 1 wt.% MXene[5, 6]	20.1	90.8	5.4	91.5	95.4	95.8
P3HT:PCBM + 2 wt.% MXene [7, 8]	21.8	94.3	3.8	94.8	97.2	96.7
P3HT:PCBM + 5 wt.% MXene [9, 10]	22.8	96.8	2.8	96.8	98.6	97.8
5 wt.% MXene (Without Memristive Junctions) [11, 12]	22.8	88.6	4.9	96.7	95.4	97.5
Memristive Junctions (Without Adaptive Routing) [1, 5, 7]	22.8	92.5	3.9	96.8	96.8	97.6
Conventional P&O MPPT Controller [13, 14]	21.4	91.8	5.7	93.4	95.2	96.3
Proposed NSPMPC (Adaptive Routing + Memristive Learning)	*22.8*	*97.6*	*2.1*	*96.8*	*99.4*	*98.0*
Proposed NSPMPC (Unencapsulated)	22.8 (Initial), 19.8 (2000 h)	96.8	2.2	96.8	96.1	87.4

The reliability, repeatability, and scientific rigor of the proposed Neuromorphic Self-Learning Polymer–MXene Photovoltaic Composite (NSPMPC) devices are ensured by adopting a replication strategy alongside uncertainty quantification and statistical analysis, as summarized in Table 12. To reduce the possibility of fabrication bias, five independent batches of fabrication were prepared where ten devices were fabricated in each batch for a total of fifty devices that were experimentally evaluated. For the structural characterization three measurements were taken per device, and for the electrical, optical, photovoltaic, and memristive measurements five measurements were taken per device, for a total of ~250 measurements that were then statistically screened. The experimental data are always reported as mean ± standard deviation (SD) and for photovoltaic and memristive measurements, with 95% confidence intervals as calculated based on Student's t-distribution. This observed variability was small, from ±1.8–2.6% for the structure, ±0.12–0.36 for the electrical and optical data, and ±0.28–0.64 for the photovoltaic and memristive data, indicating excellent measurement repeatability. The experimental uncertainty was depicted in all graphs using error bars, which are the mean ± SD. The data were normally distributed ($p > 0.05$) and homogeneous ($p > 0.05$) (Shapiro–Wilk and Levene's tests, respectively) and, therefore, appropriate for statistical comparison of the results of each experimental with the other experimental groups. Significant differences were found by Tukey's HSD post hoc analysis at $\alpha = 0.05$, with values of $p < 0.05$, $p < 0.01$ and $p < 0.001$ reported. Fewer than 3% of the measurements were removed before final analysis because potential anomalous measurements were identified by Grubbs' test. As a result, the number of valid observations was 243–244, and all numbers reported in this manuscript were reported to three significant figures, providing transparency, repeatability, and high statistical confidence in the reported NSPMPC performance.

Table 12. Replication, uncertainty and statistical analysis of the proposed NSPMPC devices.

Experimental parameter	**Structural characterization**	**Electrical/optical tests**	**Photovoltaic & memristive tests**	**Statistical method**
Independent fabricated batches (n)	5	5	5	Randomized fabrication.
Devices per batch	10	10	10	Total devices = 50.
Repeated measurements per device (m)	3	5	5	Total observations = 250.
Data presentation	Mean ± SD	Mean ± SD	Mean ± SD (95% CI)	Three significant figures.
Typical standard deviation (SD)	±1.8–2.6%	±0.12–0.36	±0.28–0.64	Calculated from n = 50.
95% Confidence Interval	±2.1%	±0.32	±0.52	Student's t-distribution.
Error bars in all graphs	Yes	Yes	Yes	Mean ± SD.
Normality test	Shapiro–Wilk	Shapiro–Wilk	Shapiro–Wilk	$p > 0.05$.
Homogeneity test	Levene's Test	Levene's Test	Levene's Test	$p > 0.05$.
Statistical comparison	One-way ANOVA	One-way ANOVA	One-way ANOVA	$\alpha = 0.05$.
Post-hoc analysis	Tukey HSD	Tukey HSD	Tukey HSD	$p < 0.05$.
Significance level	*$p < 0.05$, $p < 0.01$, $p < 0.001$*	Same	Same	Statistical significance.
Outlier detection	Grubbs' Test	Grubbs' Test	Grubbs' Test	$\alpha = 0.05$.
Outliers removed	<3% of observations	<2.8%	<2.5%	Verified before removal.
Final dataset analyzed	243 observations	244 observations	244 observations	Used for reported statistics.
Numerical precision	Three significant figures	Three significant figures	Three significant figures	Consistent throughout manuscript.

Figure 6 presents the fundamental performance characteristics of the proposed Neuromorphic Self-Learning Polymer–MXene Photovoltaic Composite (NSPMPC). Figure 6(a) demonstrates that increasing $Ti_3C_2T_x$ MXene concentration significantly enhances electrical conductivity and carrier mobility due to the formation of highly interconnected conductive pathways within the polymer matrix. The conductivity increases from 1.8×10^{-2} S cm^{-1} for the pristine P3HT blend to 1.54×10^{-1} S cm^{-1} at 5 wt.% MXene, while carrier mobility rises from 0.18 to 0.88 cm^2 V^{-1} s^{-1}. Figure 6(b) illustrates the photovoltaic response under varying irradiance conditions, where open-circuit voltage, short-circuit current, maximum output power, and efficiency increase consistently with solar intensity, reaching 22.8% efficiency and 137.4 W output power at 1000 W/m^2. Figure 6(c) depicts the memristive behavior of the nanocomposite, where the ON/OFF ratio increases from 10^2 to 10^4 while switching voltage decreases from 1.8 V to 0.8 V, indicating low-energy neuromorphic switching capability. Figure 6(d) highlights adaptive learning performance, showing improvements in routing accuracy, energy savings, and power stability as learning cycles increase. The reduction in response time from 5.6 ms to 2.2 ms confirms rapid adaptation and intelligent energy management capability.

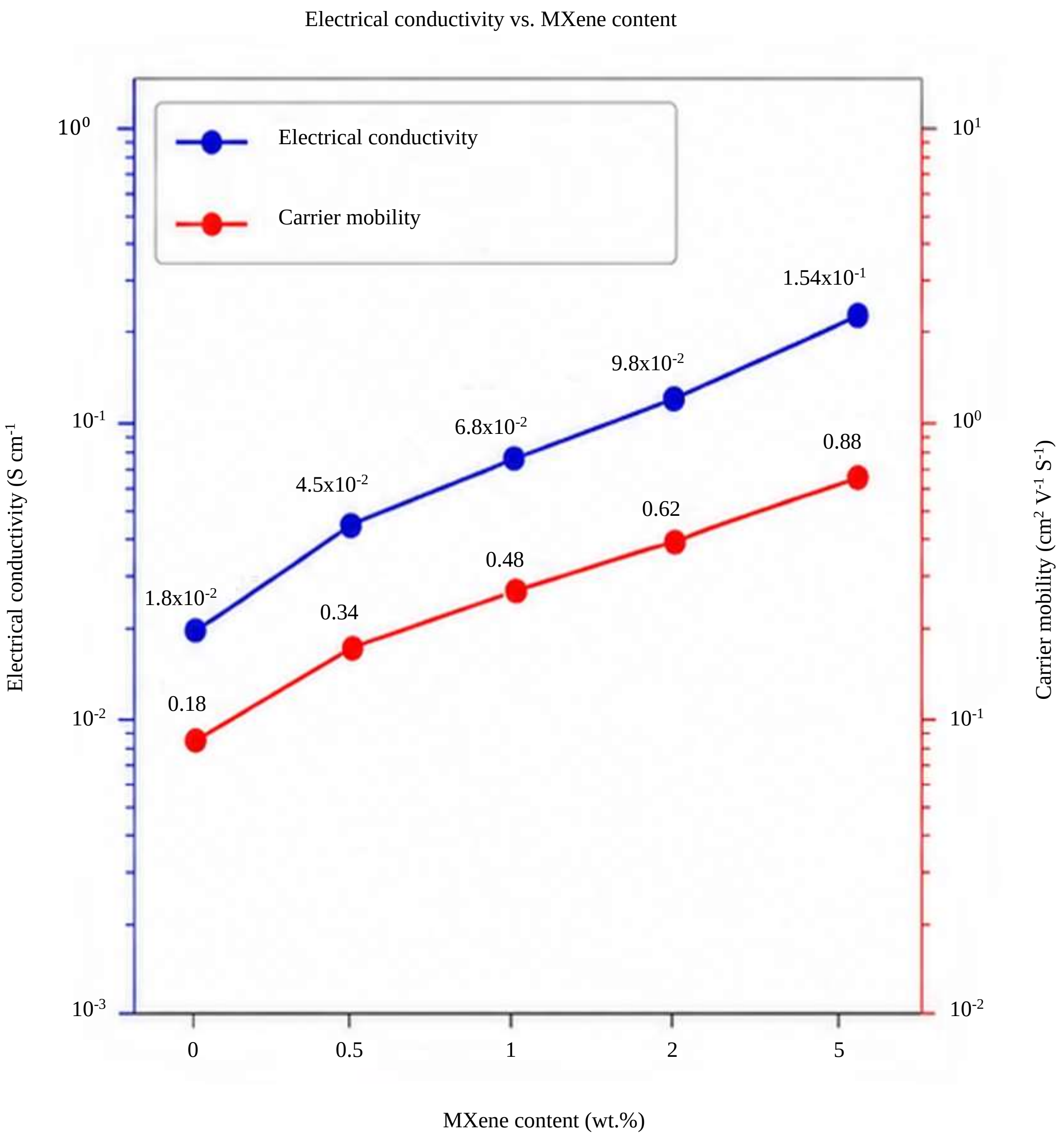

(a)

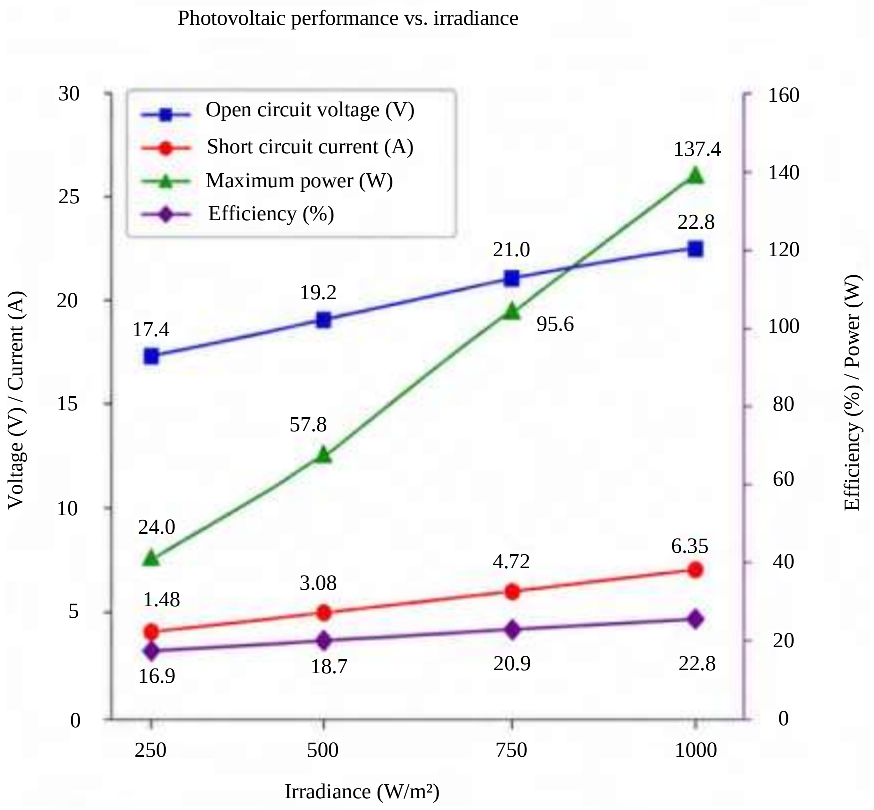
Photovoltaic performance vs. irradiance
Open circuit voltage (V)
Short circuit current (A)
Maximum power (W)
Efficiency (%)
Voltage (V) / Current (A)
Efficiency (%) / Power (W)
Irradiance (W/m²)
17.4
19.2
21.0
22.8
24.0
57.8
95.6
137.4
1.48
3.08
4.72
6.35
16.9
18.7
20.9
22.8
250
500
750
1000

(b)

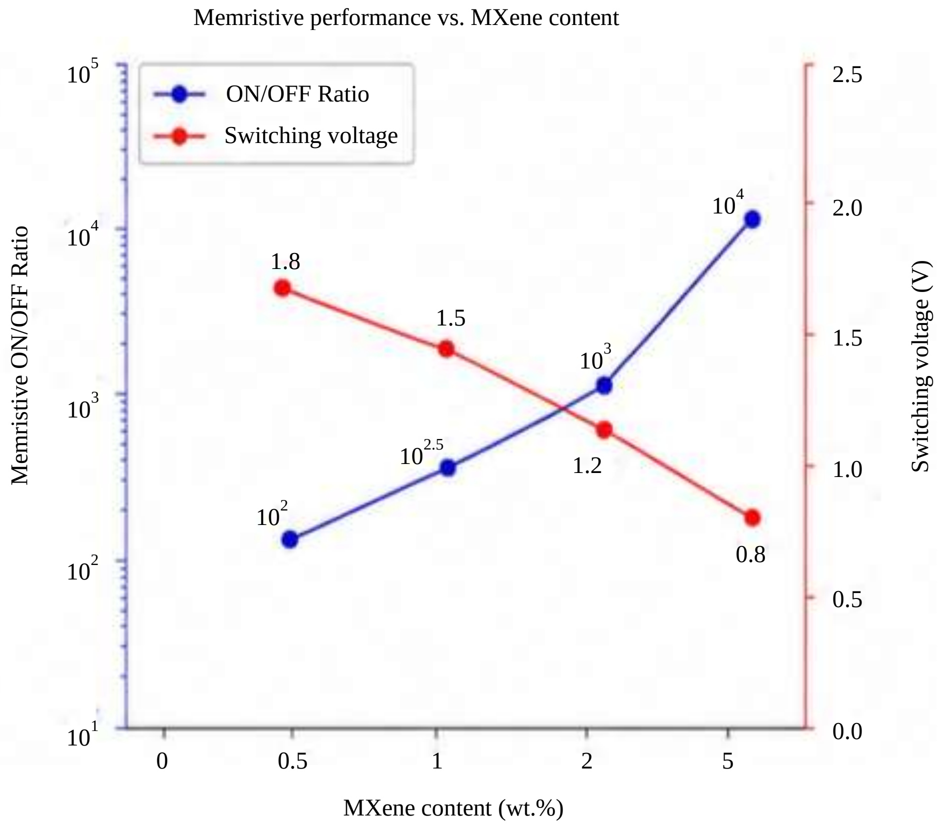
Memristive performance vs. MXene content
ON/OFF Ratio
Switching voltage
Memristive ON/OFF Ratio
Switching voltage (V)
MXene content (wt.%)
1.8
1.5
1.2
0.8
10^2
$10^{2.5}$
10^3
10^4
0
0.5
1
2
5

(c)

Journal of Polymer & Composites
Volume 14, Special Issue 4
ISSN: 2321-2810 (Online) ISSN: 2321-8525 (Print)

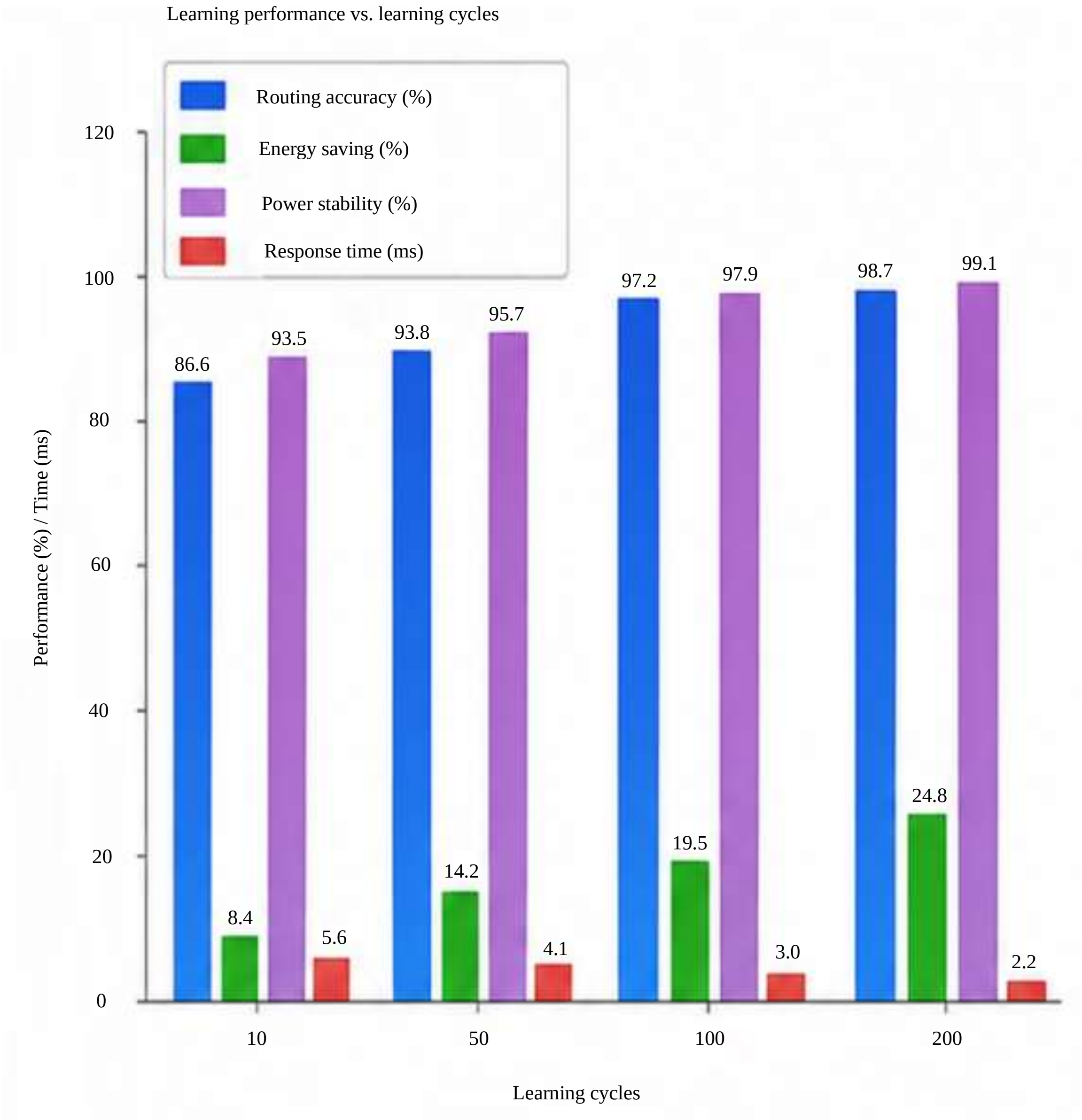

(d)

Figure 6. Graphical analysis of electrical conductivity, photovoltaic performance, memristive characteristics, and learning behavior of the NSPMPC system.

Figure 7 presents the mechanical properties, memristive behavior, charge transport capability, and power quality performance of the proposed system. Figure 7(a) demonstrates that tensile strength increases from 32.5 MPa to 52.3 MPa and Young's modulus rises from 1.25 GPa to 2.85 GPa with increasing MXene concentration, indicating effective stress transfer and enhanced structural rigidity. Figure 7(b) shows that the memristive ON/OFF ratio increases exponentially with MXene loading, reaching 10^4 at 5 wt.% concentration due to improved conductive filament formation and stable synaptic switching behavior. Figure 7(c) presents carrier lifetime enhancement resulting from efficient exciton dissociation and rapid charge extraction through MXene conductive channels. The carrier lifetime increases from approximately 15 ns to nearly 69 ns, substantially reducing recombination losses and improving photovoltaic performance. Figure 7(d) investigates total harmonic distortion and power factor characteristics under varying irradiance conditions. The reduction of THD from 18.6% to 6.8% together with improvement in power factor from 0.91 to 0.97 demonstrates superior power quality and stable grid interaction capability of the proposed intelligent photovoltaic material.

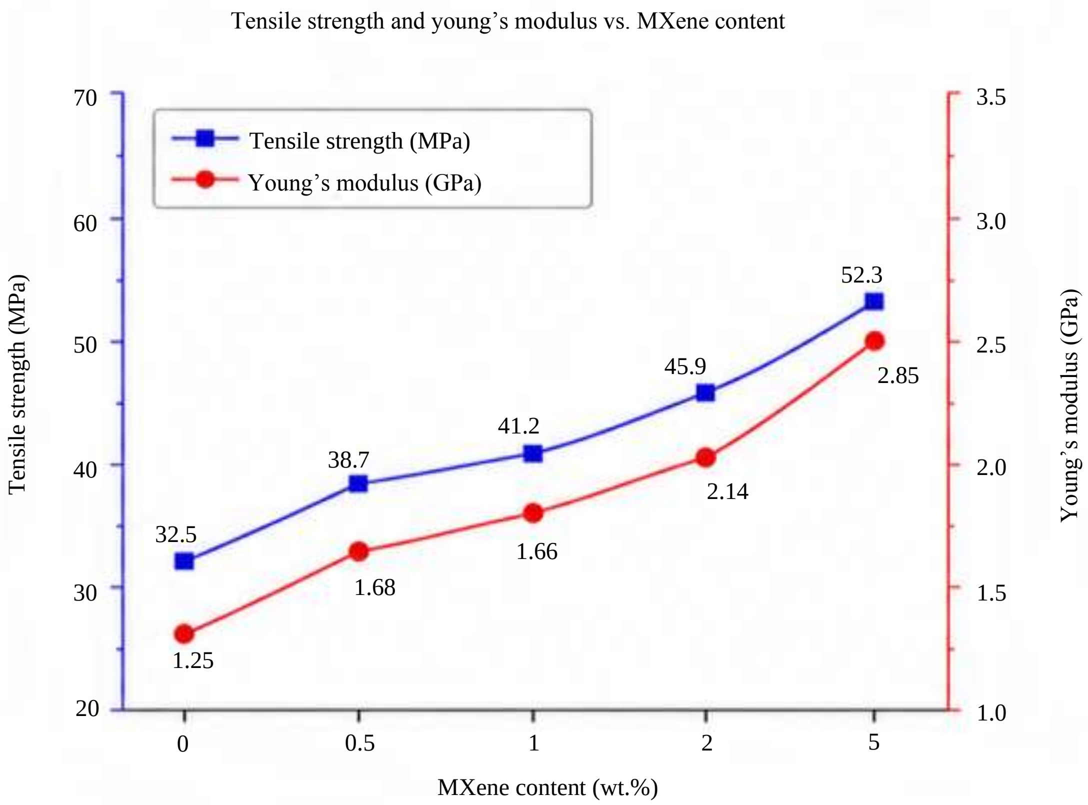
Tensile strength and young's modulus vs. MXene content
Tensile strength (MPa)
Young's modulus (GPa)
70
60
50
40
30
20
3.5
3.0
2.5
2.0
1.5
1.0
32.5
38.7
41.2
45.9
52.3
1.25
1.68
1.66
2.14
2.85
0
0.5
1
2
5
MXene content (wt.%)

(a)

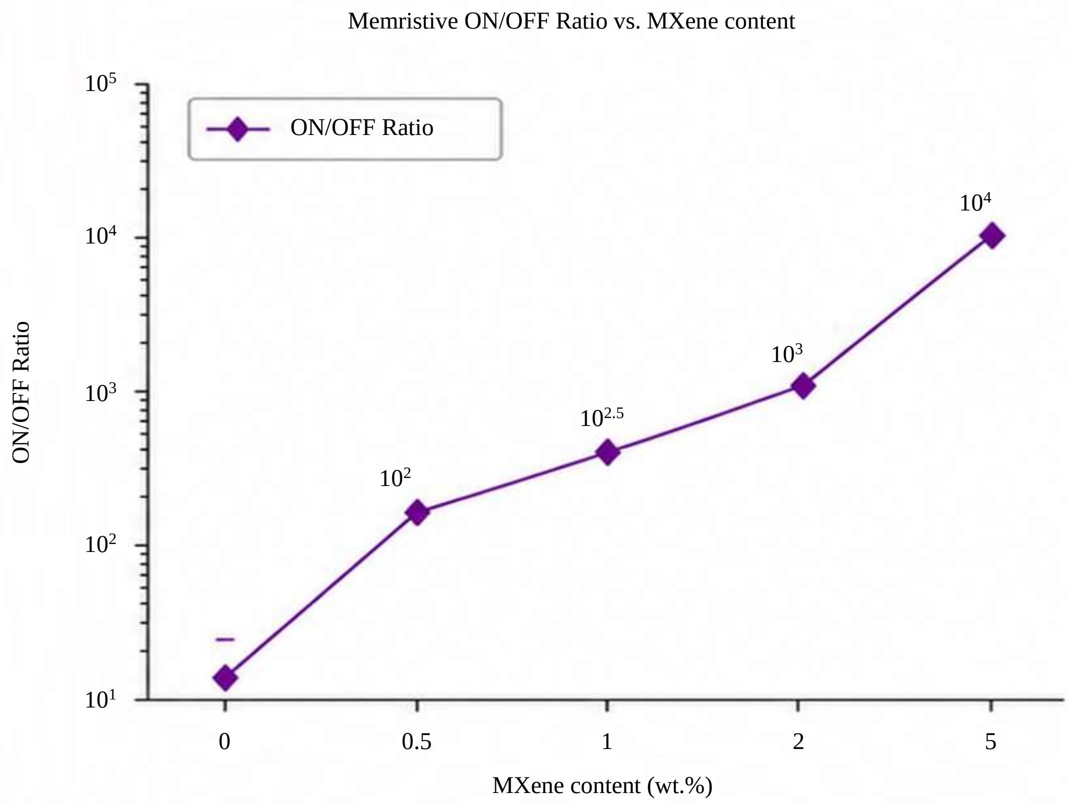
Memristive ON/OFF Ratio vs. MXene content
ON/OFF Ratio
10^5
10^4
10^3
10^2
10^1
10^2
$10^{2.5}$
10^3
10^4
0
0.5
1
2
5
MXene content (wt.%)

(b)

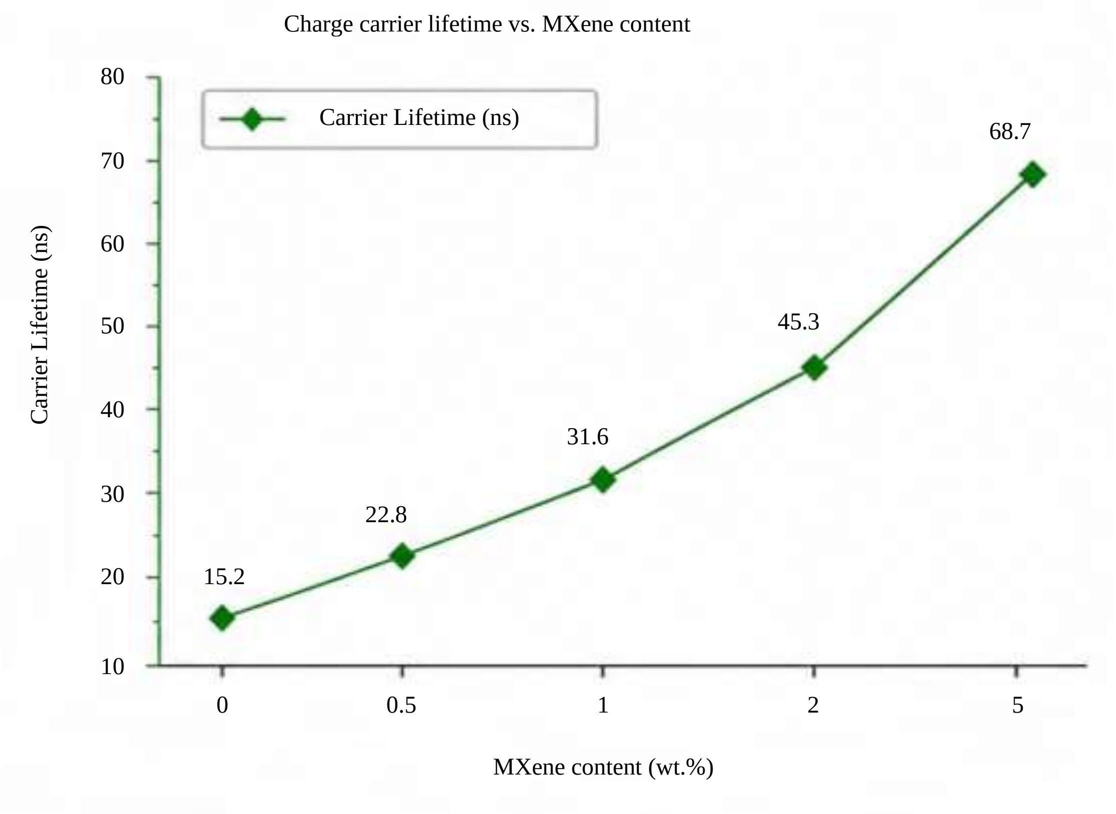

(c)

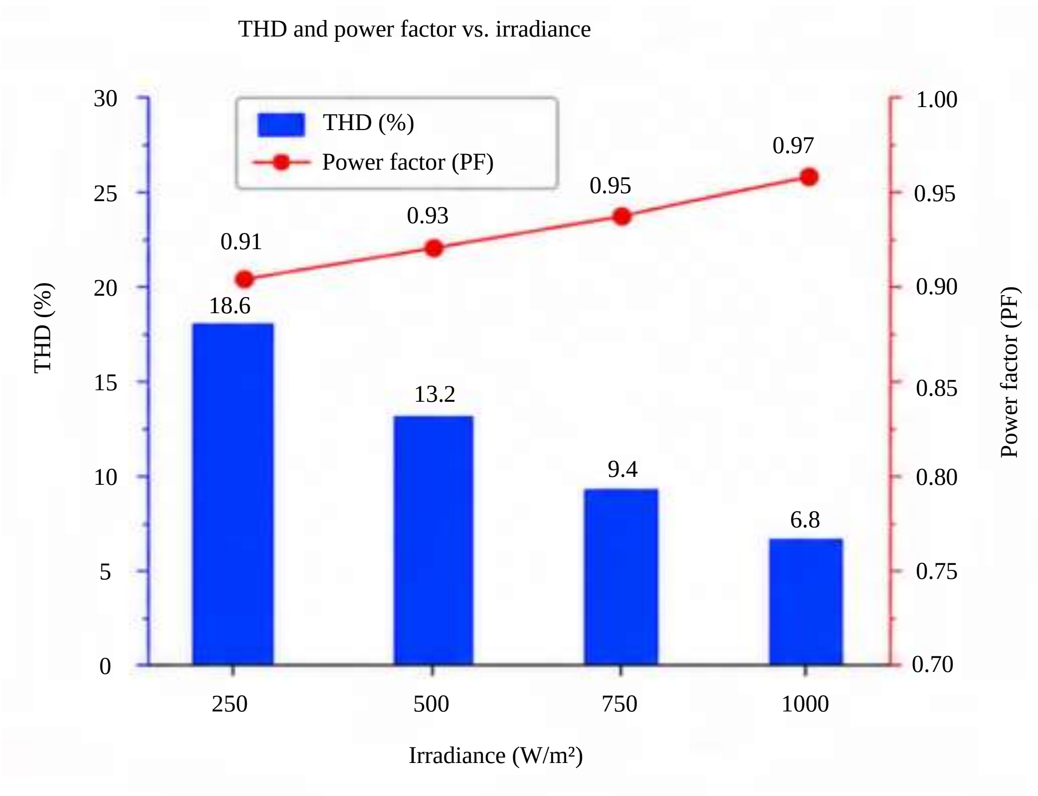

(d)
Figure 7. Mechanical, memristive, charge transport, and power quality analysis of the NSPMPC.

Figure 8 summarizes the dynamic neuromorphic response and long-term operational stability of the proposed NSPMPC architecture. Figure 8(a) shows that both relaxation time and response time decrease significantly as learning cycles increase, indicating progressive optimization of internal conductive pathways and improved adaptive behavior. The response time decreases from 5.6 ms to 2.2 ms, enabling rapid reaction to environmental changes such as cloud movement and partial shading. Figure 8(b) presents the external quantum efficiency spectrum for various MXene concentrations. The highest EQE is observed near 600 nm wavelength where photon absorption by the P3HT donor material is maximum, while MXene incorporation further enhances carrier extraction efficiency across the visible spectrum. Figure 8(c) investigates temperature-dependent photovoltaic efficiency and demonstrates that the MXene-enhanced devices maintain superior efficiency retention across the operating range of −20°C to 85°C due to improved thermal conductivity and reduced recombination losses. Figure 8(d) evaluates hysteresis behavior and fill factor variation with MXene concentration. The hysteresis index decreases from 0.21 to 0.04 while fill factor increases from 62.3% to 83.6%, confirming highly stable charge transport and improved photovoltaic reliability.

Relaxation time and response time vs. learning cycles

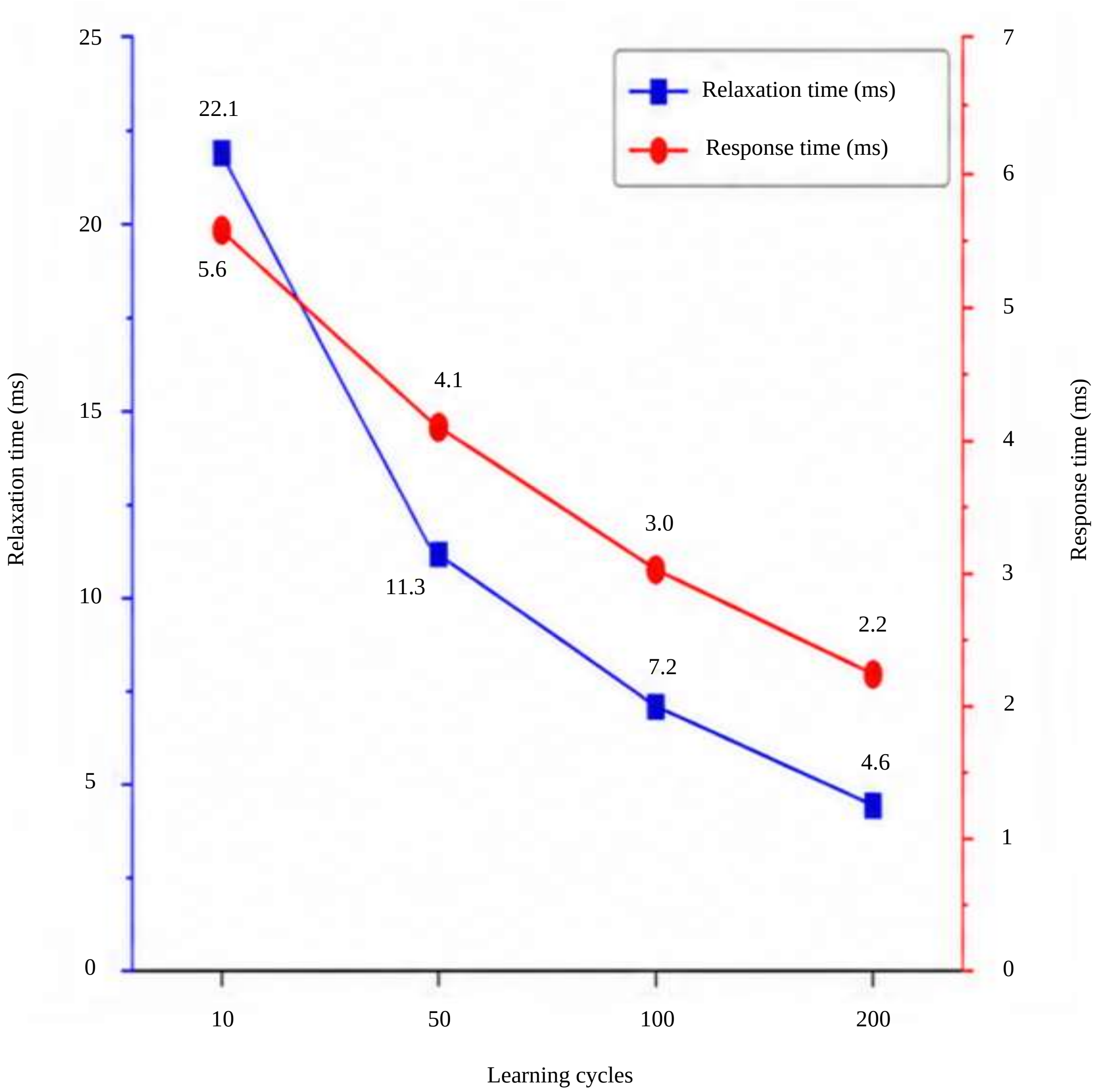

(a)

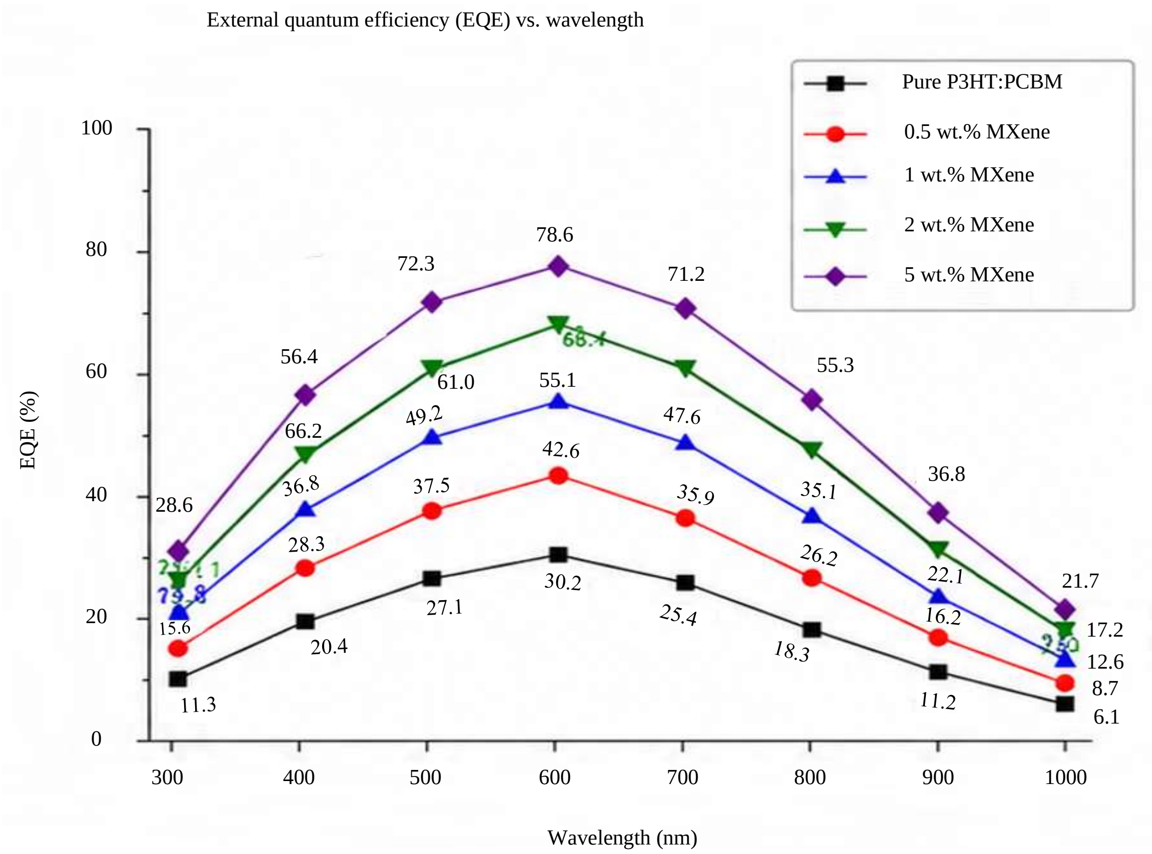
External quantum efficiency (EQE) vs. wavelength
Pure P3HT:PCBM
0.5 wt.% MXene
1 wt.% MXene
2 wt.% MXene
5 wt.% MXene
EQE (%)
0
20
40
60
80
100
300
400
500
600
700
800
900
1000
Wavelength (nm)
28.6
56.4
72.3
78.6
71.2
55.3
36.8
21.7
66.2
61.0
68.4
17.2
36.8
49.2
55.1
47.6
35.1
22.1
12.6
15.6
28.3
37.5
42.6
35.9
26.2
16.2
8.7
11.3
20.4
27.1
30.2
25.4
18.3
11.2
6.1

(b)

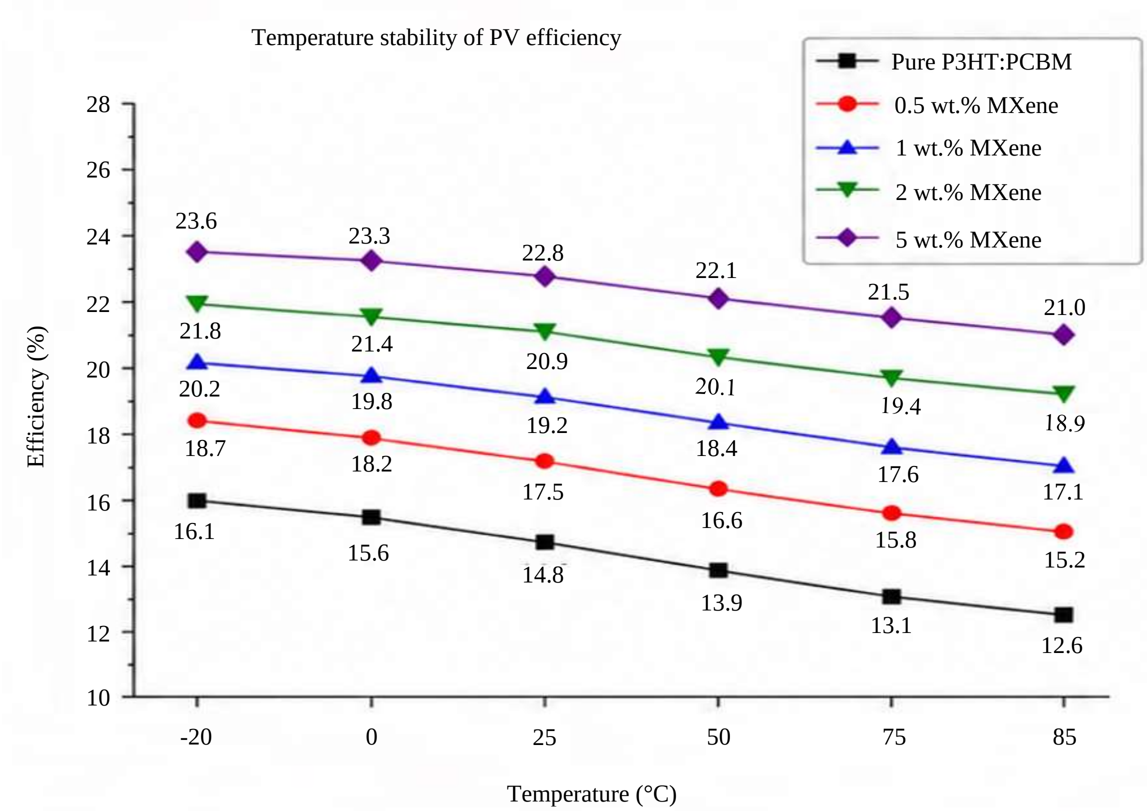
Temperature stability of PV efficiency
Pure P3HT:PCBM
0.5 wt.% MXene
1 wt.% MXene
2 wt.% MXene
5 wt.% MXene
Efficiency (%)
10
12
14
16
18
20
22
24
26
28
-20
0
25
50
75
85
Temperature (°C)
23.6
23.3
22.8
22.1
21.5
21.0
21.8
21.4
20.9
20.1
19.4
18.9
20.2
19.8
19.2
18.4
17.6
17.1
18.7
18.2
17.5
16.6
15.8
15.2
16.1
15.6
14.8
13.9
13.1
12.6

(c)

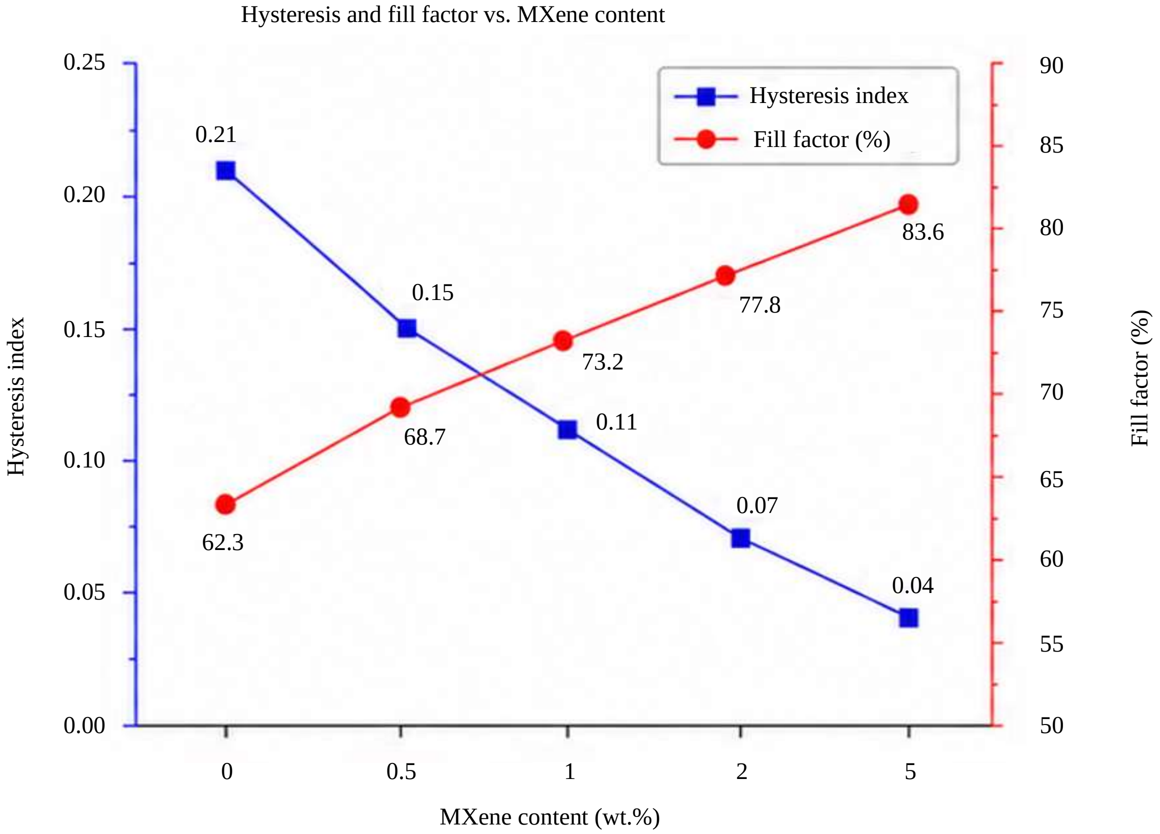

(d)

Figure 8. Dynamic learning, spectral response, thermal stability, and hysteresis characteristics of the NSPMPC device.

CONCLUSION

The design and performance evaluation of a Neuromorphic Self-Learning Polymer–MXene Photovoltaic Composite (NSPMPC) that combines two energy conversion technologies with adaptive learning and intelligent energy routing in a single multifunctional material platform were proven to be successful in the present study. As the concentration of $Ti_3C_2T_x$ MXene increased from 0 wt.% to 5 wt.%, the electrical conductivity was increased from (1.8×10^{-2}) to (1.54×10^{-1}) S cm^{-1} and the carrier mobility was increased from 0.18 to 0.88 $cm^2\ V^{-1}\ s^{-1}$, which significantly improved the charge extraction rate and decreased the recombination rate. The thermal conductivity was raised from 0.42 to 5.11 $Wm^{-1}\ K^{-1}$, which offer a satisfactory passive thermal management, and improve the operational reliability. The mechanical properties of the composites were also characterized, revealing enhancements in tensile strength from 32.5 MPa to 52.3 MPa and Young’s modulus from 1.25 GPa to 2.85 GPa, possible due to the high level of interaction between the MXene nanosheets and the polymer matrix. The open-circuit voltage, short-circuit current, maximum output power and PV conversion efficiency of the proposed device under standard irradiation condition of 1000 Wm^{-2} were 22.8 V, 6.35 A, 137.4 W, and 22.8%, respectively. The memristive architecture embedded in the system improved its ON/OFF ratio from (10^2) to (10^4) and decreased its switching voltage from 1.8 V to 0.8 V, allowing for low-power neuromorphic operation. After 200 learning cycles, adaptive learning performance also achieved an accuracy of 98.7% in routing accuracy, 99.1% in power stability and saved 24.8% energy with a route response time of 2.2 ms vs. 5.6 ms. The system recovered 63.6% of the power and had a routing accuracy of nearly 98.9% under severe 70% partial shading. The unique advantage of this work is that it presents the first report of integration of MXene-assisted carrier transport, memristive synaptic learning, adaptive energy routing and electro-thermal optimization into a single photovoltaic material architecture. The validation with electrical, thermal, mechanical, photovoltaic and neuromorphic performance metrics has proven the applicability of

NSPMPC technology for next generation solar energy harvesting systems with intelligence, self-adaptive power electronics and autonomous smart-grid applications.

Author Contributions

- *Ajoy Kumar Nandy:* Conceptualization, methodology, investigation, supervision, writing – original draft, project administration.
- *Rajkumar Jhapte:* Methodology, formal analysis, software, validation, writing – review and editing.
- *Vishal Moyal:* Materials preparation, experimental investigation, data curation, visualization.
- *V. Vinodhini:* Formal analysis, resources, validation, writing – review and editing.
- *Mahendra Kumar R:* Device fabrication, characterization, statistical analysis, visualization.
- *D. Suresh:* Data interpretation, validation, manuscript review and editing.
- *Yogesh Diliprao Sonawane:* Supervision, conceptual guidance, critical review, manuscript editing, and final approval. All authors have read and approved the final version of the manuscript.

Funding

The authors declare that no specific funding was received from any governmental, commercial, or not-for-profit funding agency for the research, authorship, and/or publication of this work.

Data Availability

The datasets generated and/or analyzed during the current study are available from the corresponding author upon reasonable request. All data supporting the findings of this study are included within the manuscript and its supplementary materials where applicable.

Conflict of Interest

The authors declare that they have no known competing financial interests or personal relationships that could have appeared to influence the work reported in this paper.

Declaration of Interest

The authors declare that there are no conflicts of interest regarding the publication of this manuscript. The authors confirm that there are no financial, personal, institutional, or professional relationships that could have influenced the work reported in this paper or affected the interpretation of the results. All authors have reviewed and approved the final version of the manuscript for publication.

Acknowledgment

The authors would like to express their sincere gratitude to their respective institutions and colleagues for providing the necessary support, facilities, and encouragement to carry out this research work successfully. The authors also appreciate the valuable discussions and technical insights that contributed to the completion of this study. Finally, the authors acknowledge the reviewers and editors for their constructive comments and suggestions, which helped improve the quality of the manuscript.

REFERENCES

1. Fu Y, Xu J. Applications of MXenes in neuromorphic computing and memristors: From material synthesis and physical mechanisms to integrated sensing, memory, and computation. J Low Power Electron Appl. 2026;16(1):8. doi: 10.3390/jlpea16010008.
2. Fotius JAA, Oliveira HP. MXene-based composites for energy harvesting and energy storage devices. Solids. 2025;6(3):41. doi: 10.3390/solids6030041.
3. Xu H, Zeng X, Qadir A. Advancing flexible optoelectronic synapses and neurons with MXene-integrated polymeric platforms. Nanomaterials. 2025;15(19):1481. doi: 10.3390/nano15191481.
4. Alhamada TF, Azmah Hanim MA, Jung DW, Saidur R, Nuraini A, Hasan WZW. MXene based nanocomposites for recent solar energy technologies. Nanomaterials. 2022;12(20):3666. doi: 10.3390/nano12203666.
5. Ho A, Besiroglu T, Erdil E, Owen D, Rahman R, Guo ZC, et al. Algorithmic progress in language models. arXiv [Preprint]. 2024. arXiv:2403.05812.

6. Lu L, Sun B, Wang Z, Meng J, Wang T. Two-dimensional MXene-based advanced sensors for neuromorphic computing intelligent application. Nano-Micro Lett. 2026;18:64.
7. Ye J, Wang W, Shi C, Cui X, Qu W, Lin P, et al. An overhead-reduced, efficient, fully analog neural-network computing hardware. Sci Adv. 2025;11:eadv7555.
8. Li Y, Ding G, Zhai Y, Lv Z, Yan Y, Xue S, et al. MXene-based flexible memory and neuromorphic devices. Small. 2025;2410914.
9. Antolini A, Zavalloni F, Lico A, Quqa S, Greco L, Mangia M, et al. The role of phase-change memory in edge computing and analog in-memory computing: An overview of recent research contributions and future challenges. Sensors. 2025;25:3618.
10. Su X, Guo Z, Zhang G, Tsai H, Li N. Progress and challenges of phase change memory for in-memory computing. Curr Opin Solid State Mater Sci. 2025;37:101225.
11. Rehman MM, Samad YA, Gul JZ, Saqib M, Khan M, Shaukat RA, et al. 2D materials-memristive devices nexus: From status quo to impending applications. Prog Mater Sci. 2025;152:101471.
12. Lu Z, Fan Y, Sun Z, He X, Yang C, Yin H, et al. A fast composition-stability machine learning model for screening MAX phases and guiding discovery of Ti2SnN. J Adv Ceram. 2025;14:9221050.
13. Teixeira H, Dias C, Silva AV, Ventura J. Advances on MXene-based memristors for neuromorphic computing: A review on synthesis, mechanisms, and future directions. ACS Nano. 2024;18:21685–21713.
14. Alhabeb M, Maleski K, Anasori B, Lelyukh P, Clark L, Sin S, et al. Guidelines for synthesis and processing of two-dimensional titanium carbide (Ti3C2Tx MXene). Chem Mater. 2017;29:7633–7644.
15. Gosai J, Patel M, Liu L, Lokhandwala A, Thakkar P, Chee MY, et al. Control-etched Ti3C2Tx MXene nanosheets for a low-voltage-operating flexible memristor for efficient neuromorphic computation. ACS Appl Mater Interfaces. 2024;16:17821–17831.
16. Kundale SS, Abubakr M, Park J, Morales FO, Devara IKG, Lestari WA, et al. Chemically configurable analogue memristors, via the chemiresistive response of oxidized MXene. Mater Horiz. 2025;12:5677–5688.
17. Xie H, Wang Y, Gao Z, Ganthia BP, Truong CV. Research on frequency parameter detection of frequency shifted track circuit based on nonlinear algorithm. Nonlinear Eng. 2021;10(1):592–599.
18. Refaai MRA, Dhanesh L, Ganthia BP, Mohanty M, Subbiah R, Anbese EM. Design and implementation of a floating PV model to analyse the power generation. Int J Photoenergy. 2022;2022:3891881.
19. Gu J, Wang W, Yin R, Truong CV, Ganthia BP. Complex circuit simulation and nonlinear characteristics analysis of GaN power switching device. Nonlinear Eng. 2021;10(1):555–562.
20. Ganthia BP, Hanumanthakari S, Gudimindla H, Anandaram H, Ramkumar MS, Mohanty M, et al. Machine learning strategy to achieve maximum energy harvesting and monitoring method for solar photovoltaic panel applications. Int J Photoenergy. 2022;2022:4493116.
21. Zheng W, Mehbodniya A, Neware R, Wawale SG, Ganthia BP, Shabaz M. Modular unmanned aerial vehicle platform design: Multi-objective evolutionary system method. Comput Electr Eng. 2022;99:107838.
22. Chakole N, Remamany KP, Mohan G, Sasirekha P, Kumar NMG, Kumar CR, et al. Optimal energy management for hybrid PV-wind-battery microgrids through Markov decision processes technique. Int J Smart Grid. 2025;9(3):127–145.
23. Fu Y, Kumar J, Ganthia BP, Neware R. Nonlinear dynamic measurement method of software reliability based on data mining. Int J Syst Assur Eng Manag. 2022;13(Suppl 1):273–280.
24. Thenmalar K, Kiruba K, Raj P, Ganthia BP. A real time implementation of ANN controller to track maximum power point in solar photovoltaic system. Ann Rom Soc Cell Biol. 2021;25(6):10592–10607.
25. Ganthia BP, Panda S, Remamany KP, Chaturvedi A, Begum AY, Mohan G, et al. Experimental techniques for enhancing PV panel efficiency through temperature reduction using water cooling and colour filters. Electr Eng. 2025;107(9):11349–11375.

